MIDI Optical Path Differences and Phases

Richard J. Mathar*
Sterrewacht Leiden, P.O. Box 9513, 2300 RA Leiden, The Netherlands
(Dated: April 7, 2006)

Although the terminology of optical path differences in the VLTI nomenclature is concealed by an almost arbitrary reference to some beam enumeration in the VLTI laboratory, the FITS tables produced by the VLTI/MIDI interferometer contain all the information to interpret the motions of the internal and main delay line mirrors unambiguously. The text is arranged in a "Q&A" fashion.

Updates of this text are placed on
`http://www.strw.leidenuniv.nl/~mathar/public/matharMIDI20051110.pdf`.

Contents

---

*URL: `http://www.strw.leidenuniv.nl/~mathar`

I. OPD INFORMATION ENCODED IN MIDI FITS FILES

A. Which of the two piezos (internal delay lines) moved?

1. The motions of the two piezo-driven internal delay lines are recorded in the `LOCALOPD` column of the `IMAGING_DATA` table. Simple inspection on a case by case reveals whether the numbers in `LOCALOPD[1]` associated with beam A, or the numbers in `LOCALOPD[2]` associated with beam B changed with time. (See again [15, 1.5.6] to disentangle the definition of beam A and beam B. Throughout this text here, I use the definition introduced by the consortium [10, 17, 19], where beam A is the Western of the two beams and passes by the DLMT — which is the opposite of the nomenclature introduced later by ESO. The figure caption of [10, Fig. 1] is correct, but the description of the beam combiner reflection/transmission on page 2 of [10] should have the nomenclature swapped.) The 1-based indexing follows FITS rules; showing the data with a variety of programming languages may display them 0-based. One can actually create schedules which move both piezos at the same time as described in [15, 3.4], but the simplified interface offered through the templates to the standard observer ensures that only one of the two piezos is moving during the exposure.

2. In addition, the same information is in the `SCAN_SETUP1` binary table in each first of the split FITS files of an exposure (see App. B): only one of the `LOC_OPL` columns changes as a function of time, ie, along the table rows. A command like

   ```
   dtfits MIDI.2005-05-27T09:50:29.250.fi* | tail -30
   ```

   would reveal this information if the eclipse software has been installed on your computer. A faster way is running my `Fits2Ascii` available from
   `http://www.strw.leidenuniv.nl/~mathar/progs/Ascii2Fits.C`, or interactive inspection with fv.

3. There is a statistical bias toward moving beam A to scan fringes. This is a mere result of having defaults in some templates which the ordinary P2PP user would hardly bother to change or would not even being offered to change; it does not guarantee that this will always be the case.

The pieces of information obtained from the first two items listed above ought be consistent.

B. What is the MIDI OPD sign convention?

1. The FITS files of the instrument do not obey an OPD sign convention, because only optical path lengths (between the instrument and the star) are provided, but no differences between these. The OPLs are encoded with the correct sign convention and an arbitrary offset (which means the common distance from a tangential plane that contains the projected baseline near the Earth to the star is discarded): Moving reflecting optical surfaces (the MDL mirrors or the internal delay line mirrors) towards the star produces smaller numbers in the associated FITS binary table—consistent with [3, 3.5.3] which says that these columns ought contain the delays *applied*. (Here, *smaller* means *arithmetically smaller*, not smaller in absolute value.) Details are found in [15, 1.5.6], available in
   `http://www.strw.leidenuniv.nl/~mathar/public/matharTRE0264.ps.gz`.

2. If, however, an application wants to apply the sign convention used in the ISS [20, 3.2.6.4], [15, 1.5.6] should be consulted to calculate a number which is consistent. According to this particular definition based on which beam is closer to some wall on Paranal, the contribution of the piezo motion plus the tracking commands sent to the MDL is

   $$D = \mathrm{OPD}[2] + \mathrm{LOCALOPD}[2] - (\mathrm{OPD}[1] + \mathrm{LOCALOPD}[1] + \mathrm{DLMT})\,, \tag{1}$$

   where the (signed) value of the DLMT is found in the `INS DLMT POS` keyword in the primary header. This must be superimposed with the contribution by the blind tracking of the MDL to get a full picture of the total OPD (see Sec. I G). The value in Eq. (1) is positive if the combined action of the internal and main delay line made the OPL from the star shining through beam B to the detector longer (synonymous to: from the star shining through beam A shorter) than following from the ISS blind tracking model geometry alone.

The reason of this fixed association of FITS indices with this particular OPD sign convention is the simplicity of the feeding optics, see Sect. I D.

3. Astronomers should be aware that the OPDs *applied* carry some "intrinsic" sign which is opposite to the *external* OPDs of astronomical relevance, simply because the principal mode of operating delay lines keeps the total OPD close to the white light fringe such that the "total" OPD seen by the detector is close to zero: the OPD *applied* by one arm of the interferometer needs to be *smaller* if the OPL to the star is *larger*. In total, there are four different ways of defining this OPD (internal versus external plus an arbitrary choice of the "first" telescope) which results in two different sign conventions. Phase sign conventions add another ambiguity well known from Fourier transforms, which does not matter here.

C. Which of the two telescopes was closer to the star?

Some approaches to the answer are:

1. If one draws a line on the ground perpendicular to the baseline which cuts the baseline vector in half (an azimuth), this defines two opposite star directions along the line for which the answer is undecided, and defines two hemispheres of directions (of star azimuths) closer to the one or to the other telescope. Consider the position angles τ for the baseline directions as listed in `http://www.eso.org/observing/etc/doc/vlti/baseline/baselinedata.txt`, updated in Appendix A, where τ is counted North through East seen from the first one. A bird's view (one of these green finches' that use Paranal for a pit stop) for the case of a star declination that places it South is:

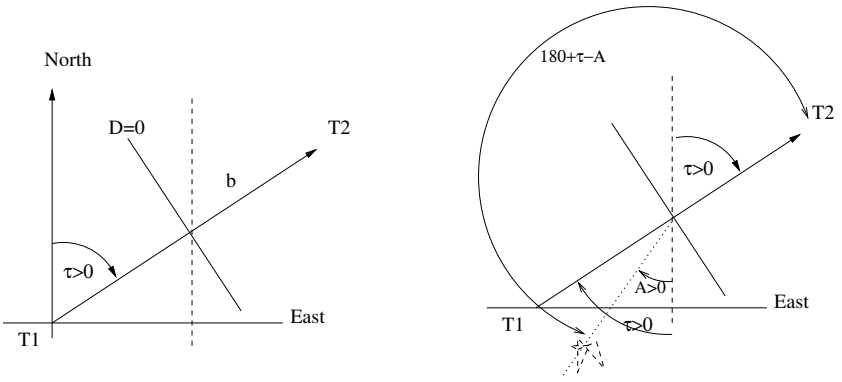

FIG. 1: In a topocentric coordinate system, the baseline direction is characterized by azimuth angles τ and $A_b \equiv \tau + 180°$. In the case shown, $0 < A < \tau < 90°$.

Further consider the azimuths A as taken from the `ESO ISS AZ` keyword in the primary header with the convention $A = 0$ for pointing to the south and $A = +90°$ for pointing to the West (see `http://archive.eso.org/Tools/DidRep/DidRepWebQuery?did=ESO-VLT-DIC.ISS` and [24, §5.1.3]. This is the standard definition on the northern hemisphere, but not the one used in [25, 3.2.1] and [9]). T_1 sees T_2 under the azimuth angle $180° + \tau$. A simple way to extract this number A is

```
dfits MIDI*.fits | egrep '(AZ|ARCFILE)'
```

with the `eclipse` software, or

```
fitshead MIDI*.fits | egrep '(AZ|ARCFILE)'
```

where available. A combined conclusion is: the star is closer to the first (left) telescope in the table if

$$|180° + \tau - A| > 90°, \tag{2}$$

else closer to the second telescope. The formula is valid for the normalizations $0 \le A \le 360°$ and $-180° \le \tau \le 180°$. With a definition

$$A_b \equiv 180° + \tau \tag{3}$$

for the baseline azimuth, it could also be written

$$|A_b - A| > 90^\circ, \quad 0 \le A, A_b \le 360^\circ. \tag{4}$$

2. The small numbers spread in the four `issgui` PostScript files of `http://www.strw.leidenuniv.nl/~mathar/prima/` show the signed external delay in meters as a function of azimuth and elevation for all station pairs where the finite range of the delay lines may render some portion of the sky not reachable (in the sense of placing the ZOPD near a common point in the interferometric lab).

3. The Java applet in `http://www.strw.leidenuniv.nl/~mathar/prima/prErrWeb.html` has a well defined (but again arbitrary) sign convention as documented. It can be fed with the FITS keywords `RA`, `DEC` and `LST` of an existing primary header plus a pair of Paranal stations and emits a signed number. (Well, it does this in parallel for two stars and emits two numbers. It is more efficient this way because the universe is quiet big and has a lot of stars [2].) This number is larger than zero if the external path length from the star to what is called `T1` in the applet is larger than the (external) path length to `T2`.

4. The interactive GUI by the Astrometric Preparation Software `http://obswww.unige.ch/~segransa/apes/prototype.html` can probably be used as well: click on the second `Start Applet` — the one below the `APES (prototype)` — chose baselines by clicking on `Select Base Line` and star coordinates by clicking on `Tutorial`. Opening an additional window under "Additional Stuff" shows a signed OPD... I do not know which sign convention is used there.

5. One can compute the product of equations (12) and (13) as formulated in (14). The variable D used there is larger than zero and the angle θ smaller than 90° if the star is closer to T2.

The results of any of these approaches ought be consistent. All but one are redundant.

D. Which of the two telescopes collected beam A, which beam B?

By following the right angle turns of the 18 mm beams back we find:

1. Moving from the ARAL feeding optics [25, 4.5.4] [20, Fig 3.8.2-1] to the MIDI warm bench, beam A was the Western one.

2. Before hitting the ARAL feeding optics, beam A was the Northern one, beam B the Southern one.

Translation into the language of the "lab input beams" of [24, 3.2], the input beam number of beam A is larger than the input beam number of beam B, both ranging between 1 and 8 (once all DLs have been installed). By reverse lookup of the numbers of the two primary header keywords `ESO ISS CONF INPUT1` and `ESO ISS CONF INPUT2`, one can get the information which of the two input beam numbers was coupled to the "first" and which to the "second" telescope. Then forward lookup with the keywords `ESO ISS CONF STATION1` and `ESO ISS CONF STATION2` gives the (station) names in the familiar nomenclature [25, Table 3-2]. Example:

```
HIERARCH ESO ISS CONF INPUT1 =    1       / Input channel in lab
HIERARCH ESO ISS CONF INPUT2 =    3       / Input channel in lab
HIERARCH ESO ISS CONF STATION1= 'U3     ' / Station of telescope 1
HIERARCH ESO ISS CONF STATION2= 'U1     ' / Station of telescope 2
```

Here $3 > 1$, therefore `INPUT2` belongs to beam A. Therefore we have to follow the entry for `STATION2` which tells us that `U1` fed beam A.

E. Was the OPL of beam A longer than the OPL of beam B?

To the precision available from variables in the primary header, this question cannot be answered, since (see above) the *external* additional OPL to the telescope further away from the star is almost equally added to the other beam by the MDL while tracking the fringe. "Almost equally" means that dispersion effects in the air-filled delay lines, lensing by the Earth's atmosphere etc [23] cause this to be true only for one "effective" point in the star spectrum.

If the question was in the sense of "Did beam A or beam B come from the telescope further away from the star?" the answer given by first answering the question in Section I D and moving with this answer on to Section I C.

F. Did the MDL passed by beam A or the one passed by beam B move?

As discussed in Section I A, `LOCALOPD[1]` or `LOCALOPD[2]` in equation (1) may change with time, `LOCALOPD[1]` always associated with beam A and `LOCALOPD[2]` always with beam B. The equivalent statement in *not* correct for `OPD[1]` and `OPD[2]`, which means if for example `OPD[1]` does not change in time but `OPD[2]` does, nevertheless the MDL passed by beam A may be the one that moves, whereas the MDL passed by beam B may be standing (then baptized the "reference" DL). The MIDI software ensures that equation (1) remains correct, although the time-dependent numbers may have been swapped from `OPD[1]` to `OPD[2]` or the other way round, including a change in sign.

If the two telescopes are on different East-West sides of the tunnel, the two MDL are also on different sides [25, 3.2.3.2.4]; see [25, Fig 3-2] or [25, Fig 3-6] to figure out whether this is currently the case: UT1, UT2 and ATs on rails A–G are West-side, whereas UT3, UT4 and ATs on rails H–M are East-side. By looking at the keyword `DEL REF NAME` and with the enumeration of [25, Fig 3-6] one can quickly explore which of the two MDLs moved for this case. Example: if `DEL REF NAME = 'DL3'`, the MDL associated with one of the East-side stations was *not* moving, neither for blind tracking nor for the commanded offsets stored in the `OPD[]`.

However, if the current telescope pair was UT3+UT4 (both with larger U coordinates than the VLTI complex and both "East-side" telescopes), this information would still not tell whether DL3 was associated with UT3 or UT4 for a full answer, even though both delay line names are provided in `ESO ISS CONF DL1` and `ESO ISS CONF DL2`. In this case one may get the information needed from a model of the change of the external OPD with time; from there, the change of the OPL reported by `DEL DLT1 OPL END`, `DEL DLT1 OPL START`, `DEL DLT2 OPL END`, and `DEL DLT2 OPL START`—one pair constant the other one the relevant one— may be either showing an increase or decrease. This sign of the time derivative of the `DEL DTLi OPL` that moved encodes implicitly whether the MDL moved that was associated with the telescope closer to the star, or the one associated with the telescope further away from the star.

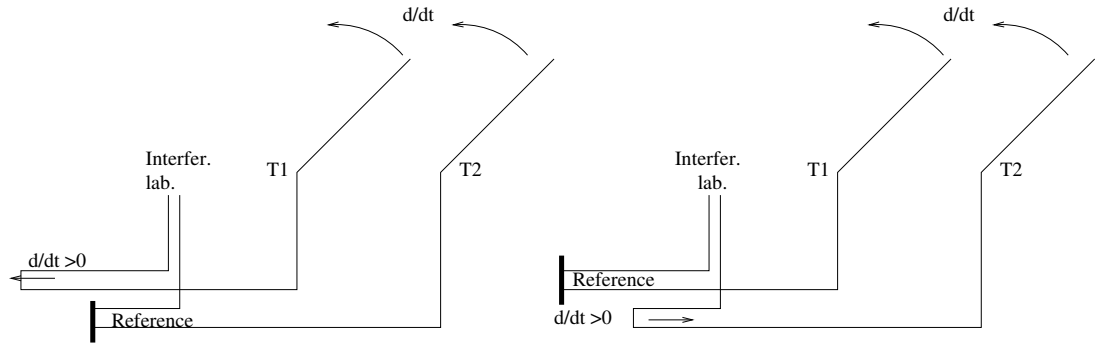

FIG. 2:

Fig. 2 shows two situations with a star moving closer to T_1 as a function of time, indicated by the curved arrows above the telescopes. On the left, the lower main delay line (the "reference") does not move and the upper one needs to move to the left to "stay on the fringe." On the right, the role of the active and reference delay lines was swapped, and the lower delay line must move to the right as a function of time. We may assume that both delay line positions refer to coordinate systems that provide a (positive) relative distance to the facing/opposite wall, which means that the sign of the time derivative of the MDL positions differs in the two cases.

The GUI `prErrWeb.html` mentioned in Section I C shows the external OPD and also its time derivative. In the graph above and with the sign convention used in the GUI, the OPD of the graph is positive and its time derivative negative; it is eventually the quotient of dD/dt by the time derivative off the moving MDL position (both of approximately the same absolute value) which matters: if close to -1, the MDL of T_1 moves, if close to $+1$, the MDL of T_2.

G. What was the actual external OPD?

The quickest way to compute the unsigned OPD $|D|$ is to use the vector equation $\mathbf{D} = \mathbf{b} - \mathbf{P}$ in the form

$$D^2 = b^2 - P^2. \tag{5}$$

The baseline length b could be obtained

- according to $b^2 = (\mathrm{T1X}-\mathrm{T2X})^2+(\mathrm{T1Y}-\mathrm{T2Y})^2+(\mathrm{T1Z}-\mathrm{T2Z})^2$ with values extracted from the primary header keywords `ESO ISS CONF T1X` etc or from the column `STAXYZ` in the table `ARRAY_GEOMETRY`.
- from the web page `http://www.eso.org/observing/etc/doc/vlti/baseline/baselinedata.txt` .
- via the geographical coordinates Φ and λ of App. G 1, which are equivalent to the angle of separation Z between the two telescopes subtended at the center of the Earth, using [16]:

$$b = \rho\sqrt{2(1-\cos Z)} = 2\rho\sin\frac{Z}{2} \approx \rho\left(Z - \frac{Z^3}{24} + \frac{Z^5}{1920} - \cdots\right), \tag{6}$$

$$\cos Z = \sin\Phi_1\sin\Phi_2 + \cos\Phi_1\cos\Phi_2\cos(\Delta\lambda). \tag{7}$$

A numerically stable evaluation would insert the Taylor expansion

$$2(1-\cos Z) \approx (\Delta\Phi)^2 + \cos^2\Phi_2(\Delta\lambda)^2 - \frac{\sin(2\Phi_2)}{2}\Delta\Phi(\Delta\lambda)^2 - \frac{\cos^2(\Phi_2)}{2}(\Delta\Phi\Delta\lambda)^2 - \frac{1}{12}(\Delta\Phi)^4 - \frac{\cos^2\Phi_2}{12}(\Delta\lambda)^4 \tag{8}$$

into the first equation, where $\Delta\lambda = \lambda_1 - \lambda_2$. The effective Earth sphere radius ρ includes the mountain altitude `ESO ISS GEOELEV`.

The projected baseline length P at the start and end of the exposure is listed under `ESO ISS PBL12 START` and `ESO ISS PBL12 END` in the primary header.

H. How do piezo movements relocate the point of ZOPD on the sky?

1. *Qualitative: Sign*

Sky positions of equal OPD are concentric circles on the celestial sphere centered at the baseline vanishing point, see [23, §29]. On an imaging detector, they are lines. Which of the two baseline directions points to the circle's center depends on the sign of the OPD. Change of the internal OPD augments or shrinks the radius of this circle of ZOPD, as if one would select coherent light from a different position on the sky. This changes the star azimuth A (the point where this circle touches the observer's horizon), and with equation (4) one may say that this change moves the star closer to T_1 if $|A_b - A|$ increases, or else moves the star closer to T_2 if this absolute value decreases.

Normal interferometric VLTI operation tracks the star with the MDL such that the path length L_1 from the star through T_1 to the beam combiner equals the path length L_2 through T_2 to the beam combiner. Path lengths stretch over "external" plus "internal" parts,

$$L_1 = L_2, \quad L_1 = L_1^{\mathrm{ext}} + L_1^{\mathrm{int}}, \qquad L_2 = L_2^{\mathrm{ext}} + L_2^{\mathrm{int}}. \tag{9}$$

Coherent with the rest of this script we adopt the sign convention

$$D \equiv L_1^{\mathrm{ext}} - L_2^{\mathrm{ext}} \tag{10}$$

for the external OPD. [There are four possible combinations of being closer to either telescope before the change and changing this closeness, equivalent to the "Kronecker product" of a sign in D and a sign in ΔD caused by a change in one of the L_i, and also equivalent to a sign of $|A_b - A| - 90°$ and a change of this value.] The previous two equations yield

$$\Delta D = \Delta(L_1^{\mathrm{ext}} - L_2^{\mathrm{ext}}) = \Delta(L_1 - L_2 - L_1^{\mathrm{int}} + L_2^{\mathrm{int}}) = \underbrace{\Delta(L_1 - L_2)}_{0} + \Delta(L_2^{\mathrm{int}} - L_1^{\mathrm{int}}). \tag{11}$$

If we define the MIDI piezo motion relative to its rest position, we have $\Delta L_i^{\mathrm{int}} < 0$ since it pushes the roof top mirror towards the beam during the standard "ramp" as the voltage is applied and the piezo expands. If furthermore we have a motion driven by the standard templates, this moves the beam with index $i = A$, which is to be checked as described in Section I A. Furthermore $\Delta L_A^{\mathrm{int}} < 0$ is equivalent to $\Delta L_B^{\mathrm{int}} > 0$ with respect to ΔD, or equivalent to $\Delta L_B^{\mathrm{ext}} < 0$, deduced from the equations above as the total path length is kept balanced between the two arms of the interferometer. In the nomenclature introduced above, this reduction in the external path length L_B^{ext} means the point on the sky moves towards the telescope of beam B.

2. Quantitative

We can work this out more quantitatively: We define the two geographical latitudes Φ_i and longitudes λ_i of T_1 and T_2 and from there the Cartesian coordinates of the baseline vector $\mathbf{b}_{12}$ from T_1 to T_2 [14, 16], App. F:

$$\mathbf{b}_{12} = \rho \cdot \begin{pmatrix} -\sin\Phi_1 \cos\Phi_2 \cos(\Delta\lambda) + \cos\Phi_1 \sin\Phi_2 \\ \cos\Phi_2 \sin(\Delta\lambda) \\ \cos\Phi_1 \cos\Phi_2 \cos(\Delta\lambda) + \sin\Phi_1 \sin\Phi_2 - 1 \end{pmatrix} \tag{12}$$

where $\Delta\lambda \equiv \lambda_1 - \lambda_2$, $|\mathbf{b}_{12}| = b$, where x points to the North, y to the West and z to the zenith at the location of T_1, and where $\rho \approx 6380$ km is the effective Earth radius at the platform. Alternatively, one may generate the first two components of this vector by subtracting two of the e and n numbers from `http://www.eso.org/observing/etc/doc/vlti/baseline/vltistations.html` and setting the third to zero, or using the table in [17, §6.2.1].

The star direction is

$$\mathbf{s} = \begin{pmatrix} -\cos A \sin z \\ \sin A \sin z \\ \cos z \end{pmatrix} \tag{13}$$

in the same coordinates, with the Azimuth convention of Section I C. The external delay D is the dot product

$$D = \mathbf{s} \cdot \mathbf{b}_{12} = b \cos\theta; \quad 0 \le \theta \le \pi \tag{14}$$

with the sign convention that $D > 0$ and $\cos\theta > 0$ if the star is closer to T_2 than to T_1. The cone angle θ of the circle of constant external OPD seen from the platform is

$$\cos\theta = \mathbf{s} \cdot \hat{\mathbf{b}}_{12}; \quad \hat{\mathbf{b}}_{12} \equiv \mathbf{b}_{12}/b; \quad P = b \sin\theta. \tag{15}$$

The (signed) change in OPD is related to the angular change $\Delta\theta$ of the ZOPD via the differential of (14)

$$\Delta D \approx -b \Delta\theta \sin\theta; \tag{16}$$

$$\Delta\theta \approx -\frac{\Delta D}{b \sin\theta} = -\frac{\Delta D}{P}, \tag{17}$$

where $b > 0$, $\sin\theta > 0$, $P > 0$. The recipe to calculate the signed $\Delta\theta$ is

- take P from the header as described in Section I G.
- Check as in Section I A whether the piezo of beam A or beam B moved, and obtain the local change ΔL (L is the total path length from the star to the detector. Up to some arbitrary constant, $-150\ \mu\text{m} < L^{\text{int}} < 0$, but ΔL^{int} may have both signs depending on what one defines as the reference. If the reference is the rest position, $\Delta L^{\text{int}} < 0$.)
- (Note that the next step associates L with one of the telescopes and an "internal" delay, and that there are various equivalent ways of doing this as discussed above, only one of which is picked here.) Select one of the telescopes to be T_1, the other T_2, in accordance to the choice that defines the signs of Eq. (12) and (14). Figure out as in Sect. I D whether the piezo handled the beam through T_1 or the beam through T_2. If the piezo modified the beam through T_1, flip the sign of ΔL^{int} (as to relate L to the internal delay imposed by T_2).
- Define the ZOPD as given by (11),

$$\Delta D = \Delta L^{\text{int}} \tag{18}$$

  and obtain the signed $\Delta\theta$ via (17).

The limitations for the piezo range ($|\Delta L| < 150 \times 10^{-6}$ m), the baseline ($b \ge 46.6$ m for UTs), and the zenith distance ($\theta \ge 30°$) result in the limit $\Delta\theta \le 6.4 \times 10^{-6}$ rad $= 1.3''$ obtained from (17). Larger ZOPD shifts must be relayed to the MDL.

The orthogonal projection of the change $\Delta\theta$ along the perimeter of the circle is only resolved through the PSF of the single telescope ($1.2\lambda/d = 0.31''$ for $d = 8$ m at $\lambda = 10\ \mu$m, $1.2\lambda/d = 1.38''$ for $d = 1.8$ m at $\lambda = 10\ \mu$m), the

radial direction resolved proportional to λ/P of the interferometer. One may chose to associate $\Delta\theta$ not only with a change in the distance to the baseline's line of sight, but also with a specific direction $(\Delta A, \Delta z)$ in the tangential plane to the celestial sphere attached to A and z. Then from [23, §28.3.4] (see App. E)

$$(\Delta\theta)^2 = (\Delta z)^2 + \sin^2 z(\Delta A)^2 - \frac{1+2\cos^2 z}{12}(\Delta z)^2(\Delta A)^2 - \frac{1}{12}\cos^2 z \sin^2 z(\Delta A)^4 + \cdots \tag{19}$$

The two components of the gradient are

$$\frac{\partial D}{\partial A} = \frac{\partial \mathbf{s}}{\partial A}\cdot\mathbf{b}_{12} = \begin{pmatrix} \sin A \sin z \\ \cos A \sin z \\ 0 \end{pmatrix}\cdot\mathbf{b}_{12}, \tag{20}$$

$$\frac{\partial D}{\partial z} = \frac{\partial \mathbf{s}}{\partial z}\cdot\mathbf{b}_{12} = \begin{pmatrix} -\cos A \cos z \\ \sin A \cos z \\ -\sin z \end{pmatrix}\cdot\mathbf{b}_{12} \tag{21}$$

by differentiation of (14). If one wants to calculate the direction $(\Delta A, \Delta z)$ of radial (steepest) change of the circle of ZOPD, for example, one would chose $\Delta A/\Delta z = (\partial D/\partial A)/(\partial D/\partial z)$, calculate the partial derivatives from the dot products in the previous two equations, divide (19) through $(\Delta z)^2$, and obtain Δz from (19). This approach works as well for the declination δ and right ascension α (or hour angle h) substituted for A and z in (13):

$$\mathbf{s} = \begin{pmatrix} \cos\Phi_1 \sin\delta - \sin\Phi_1 \cos\delta \cos h_1 \\ \cos\delta \sin h_1 \\ \sin\Phi_1 \sin\delta + \cos\Phi_1 \cos\delta \cos h_1 \end{pmatrix}; \quad h_1 - h_2 = \lambda_1 - \lambda_2. \tag{22}$$

The dot product $\mathbf{s}\cdot\mathbf{b}_{12}$ with (12) is

$$D = \rho(\cos\delta\cos\Phi_2\cos h_2 + \sin\delta\sin\Phi_2 - \sin\Phi_1\sin\delta - \cos\Phi_1\cos\delta\cos h_1). \tag{23}$$

$\Delta\Phi \equiv \Phi_1 - \Phi_2$ and $\Delta\lambda$ are small, measured in radian; from App. G 1 we have $|\Delta\Phi| < 2.4\times10^{-5}$ rad and $|\Delta\lambda| < 3.1\times10^{-5}$ rad, the maximum North-South distance realized by the station pair B5–J6, and the maximum East-West distance by A1–M0. To avoid the massive cancellation of digits in (23), one would use the bivariate Taylor expansion

$$\begin{aligned} D/\rho \approx\ & (\sin\Phi_2\cos\delta\cos h_2 - \cos\Phi_2\sin\delta)\Delta\Phi + \cos\delta\sin h_2\cos\Phi_2\Delta\lambda \\ & + \frac{1}{2}(\sin\delta\sin\Phi_2 + \cos\delta\cos h_2\cos\Phi_2)(\Delta\Phi)^2 - \sin\Phi_2\cos\delta\sin h_2\Delta\lambda\Delta\Phi + \frac{1}{2}\cos\delta\cos h_2\cos\Phi_2(\Delta\lambda)^2. \end{aligned} \tag{24}$$

The $\partial D/\partial\delta$ and $\partial D/\partial\alpha$ follow from there. For the details one must split the hour angle into a change in sky coordinate and a time difference $\Delta t = \Delta h + \Delta\alpha$, ie, judge to which degree the change in the piezo position has been instantaneous.

I. What does this mean for the determination of phases from MIDI?

(Section contributed by C Leinert).

Consider an object $V_\lambda(\alpha)$, where α is an angle on the sky. We write its one-dimensional Fourier transform, i.e., its complex visibility, as $\mathcal{V}_\lambda(u) = \int_{-\infty}^{\infty} V_\lambda(\alpha) e^{-2\pi i u\alpha} d\alpha = |\mathcal{V}_\lambda(u)|\, e^{i\varphi_\lambda(u)} \equiv A_\lambda e^{i\varphi_\lambda(u)}$ with visibility amplitude $A_\lambda(u)$ and phase $\varphi_\lambda(u)$. Observing this object interferometrically with a baseline of projected length P and a corresponding spatial frequency $u = P/\lambda$ on the sky leads for multiaxial beam combination to a visualisation of the visibility component $\mathcal{V}_\lambda(u)$ as an instantaneous fringe pattern in the image plane of

$$I_\lambda(x) \propto 2\,|\mathcal{V}_\lambda(u)|\cos(2\pi f_m x + \varphi_{\lambda(u)}), \tag{25}$$

where $1/f_m$ is the spatial fringe spacing. Alternatively, in coaxial beam combination this visibility component shows as an OPD-scanned timewise fringe pattern of

$$I_\lambda(D) \propto 2\,|\mathcal{V}_\lambda(u)|\sin(2\pi f_c D + \varphi_{\lambda(u)}), \tag{26}$$

where $1/f_c$ is the time interval by which the OPD changes by λ during a scan. The latter method is used in the MIDI instrument on the VLTI. The presence of the sine function in relation (26) instead of the cosine function results from the well known $\pi/2$ phase shift in the symmetrically used beam splitter which brings about the coaxial recombination;

the factor of two results from taking the difference of the two beamsplitter output signals of opposite sign. As we will see, the $\pi/2$ phase shift is of no consequence for the phase determination. The positive directions of x in (25) and D in (26) need a corresponding positive scan direction over the source on the sky. Otherwise the phase φ_λ would change sign. In other words, defining the signs of x, resp. D and keeping Eqs. (25) and (26) defines also a positive direction on the sky.

Equations (25) and (26), though plausible, deserve some justification in detail, in particular to verify the sign of the angle α and of the phases. We start from Boden's [4] presentation. A plane wave propagating from the object in direction $\mathbf{k}$ towards the observer is written as $e^{i\mathbf{k}\cdot\mathbf{x}-i\omega t}$ with $|\mathbf{k}| = k = 2\pi/\lambda$. Using telescopes A and B we define the baseline vector $\mathbf{b}$ as A $\rightarrow$ B. Pointing the telescopes to the object, we are viewing in direction $\mathbf{s} = -\mathbf{k}$. The optical path difference counted in the sense A minus B then is $D = \mathbf{s}\cdot\mathbf{b} + L_A^{\rm int} - L_B^{\rm int}$, where $L^{\rm int}$ are the path lengths from the telescopes to the locus of beam combination. From the superposition of the waves travelling through telescope A, $e^{ik(\mathbf{s}\cdot\mathbf{b}+L_A^{\rm int})-i\omega t}$, and telescope B, $e^{ikL_B^{\rm int}-i\omega t}$, the fringe pattern results as

$$I_\lambda(D) \propto \cos[k(\mathbf{s}\cdot\mathbf{b} + L_A^{\rm int} - L_B^{\rm int})]. \tag{27}$$

To relate positions on the sky to the instrumentally available OPD, we consider the viewing direction $\mathbf{s}$ as origin on the sky. We take as zero point of OPD that value of $L_A^{\rm int} - L_B^{\rm int}$ where a point source at this origin would produce the white light fringe, i.e., where the argument of the cosine in (27) is zero. Similarly, we count α positive on the sky in the direction where the corresponding white light fringes would occur at positive OPD, which means that α goes positive towards telescope A, while $\mathbf{s}\cdot\mathbf{b}$ is going negative in this direction. For an extended source we have to add the independent fringe patterns contributed from all its parts, which means integrating $\cos(-k\alpha P + kD) = \cos(2\pi\alpha P/\lambda)\cos(kD) + \sin(2\pi\alpha P/\lambda)\sin(kD)$ over α. Keeping the above definition of visibility in mind, the integral equals $|\mathcal{V}_\lambda(u)|\cos\varphi\cos(kD) - |\mathcal{V}_\lambda(u)|\sin\varphi\sin(kD)$ which directly leads to the form of (25), from which (26) follows simply by applying the $\pi/2$ phase shift. This verifies the formulation of Eqs. (25) and (26).

In MIDI, D in (26) is the actual optical path difference for a given individual exposure. One such exposure gives $I_\lambda(D)$ as function of λ for the range 8–13 μm. Many of these exposures at a repeated sawtooth pattern of OPD steps scanning the fringe constitute an interferometric measurement. In each scan, the position of fringe maximum depends on the phase φ_λ.

For later use we note that by the formulation of (26), when φ_λ is going positive from the value 0 (which a point source at the origin would have), then the maximum, respectively the zero crossing of the fringe pattern (26) at the origin will move to negative values of x, respectively OPD. We also note that with the sign conventions applied for the VLTI and MIDI (OPD = path length "MIDI beam A" minus path length "MIDI beam B"), an interferometric scan with MIDI moves the OPD stepwise towards more negative values. In the actual mechanical-geometrical setup, during such an OPD scan of the MIDI instrument the corresponding position of the sky moves towards that one of the two used telescopes that sends its light beam into the right entrance window of the MIDI dewar, when seen with the incoming light ("MIDI beam B"). The fits headers of the stored data files carry the information which allows to transpose this somewhat convolved definition into a defined direction on the sky such that the phases will give defined information on the object.

For the determination of phases from MIDI measurements it is important to realise that the optical path difference consists of two parts of different behaviour: $D = D_i + D_a$, where the "instrumental" D_i is quickly stepped through a few times the wavelength of ≈ 10 μm during an interferometric measurement and is known including its sign, while D_a is mostly determined by the atmosphere and is more slowly varying with a few μm/s, but in an unpredictable way.

The EWS part of the MIDI data reduction package determines the phase by mathematically shifting each exposure as given by (26) to OPD zero and then averaging to obtain the complex visibility—moduls and phase [12]. Remembering that a shift in image space (and here also in OPD) corresponds to a phase factor in Fourier space of the kind $e^{2\pi iuD}$, we multiply (26) by $e^{-2\pi iuD_i}$ to "shift" each exposure $I_\lambda(D)$ back to position $D_i = 0$. Equation (26) now reads—apart from factors which do not matter here—

$$I'_\lambda(D) = \frac{A_\lambda}{i} e^{2\pi iuD_a + i\varphi_\lambda} - \frac{A_\lambda}{i} e^{-4\pi iuD_i - 2\pi iuD_a - i\varphi_\lambda}. \tag{28}$$

To determine the unkown atmospheric optical path difference D_a, we Fourier transform (27) with respect to u and obtain peaks at $+D_a$ and $(-D_a - 2D_i)$. The second term of these, rapidly changing with D_i during a scan, quickly smears out by averaging over a few exposures, so the only remaining peak gives the wanted value of D_a with correct sign. We now can perform the "shifting back" correction also for the atmospheric part of the OPD by multiplying equation (27) with $e^{-2\pi iuD_a}$. This leads to

$$I''_\lambda(D) = A_\lambda e^{+i(\varphi_\lambda \pm \pi/2)}, \tag{29}$$

where we have omitted the strongly oszillating part with the factor $e^{-4\pi iuD_i - 4\pi iuD_a - i\varphi_\lambda}$. The constant $\pi/2$ results from the factor $1/i$, its sign depends on which of the two complementary interferometric signals after the beam splitter is subtracted from the other one. Averaging equation (29) over the typically several thousand exposures of an interferometric measurement thus will reliably determine—apart from a constant known in principle— the wanted phase $\varphi_\lambda(u = P/\lambda)$ over the wavelength range 8–13 μm. (At the same time, it will also give the visibility amplitude A_λ). We remove any linear trend with u from this phase, since it simply would correspond to a position offset of the source from the origin. As well we remove any remaining constant term $\neq 0$. Again apart from our constant, this term could be and appears to be mostly due to differential longitudinal dispersion over the unequally long air paths of the interfering light beams and it thus mostly carries information not related to the object. Of course, subtraction of the constant term also takes care of the added $\pm\ \pi/2$. This ends the determination of phase. We note that the data reduction procedure described here preserves the sign as given in (26).

We now consider a binary with the center of light in the origin to confirm by a detailed look at the temporal fringe pattern that the phases determined by MIDI do have the correct sign.
On the sky we are on save grounds: The phase would show the form of a staircase with width of the individual steps in spatial frequency u of $\Delta u = 1/\text{separation}$ and the height of the steps depending on the brightness ratio. The phase will decrease with u if the companion is located at more negative α with respect to the primary. On the other hand, the binary's phase with removed linear trend —as determined for the instrument MIDI—corresponds to a different position, namely with the primary at the origin. The binary phase now oscillates around zero. For a companion at more negative position than the primary, the phase will increase with u (decrease with λ) at those spatial frequency values where the maxima of the visibility amplitude are found, a simple and useful criterion. *In the instrument* it looks like this: If we have a companion at slightly negative α with respect to the primary, its contribution to the temporal fringe would have a maximum slightly later in the OPD scan, at $\Delta D_C = -\alpha P$. The maximum of the combined fringe pattern (primary plus companion) then will also be shifted to more negative values, by

$$\Delta D_B = -\alpha P \frac{F_{\text{comp}}}{F_{\text{prim}} + F_{\text{comp}}}. \tag{30}$$

Measured in units of λ, this shift will decrease in absolute value, i.e. get more positive, rise with increasing λ. The phase φ_λ, corresponding to this shift of maximum, therefore will get more negative, decrease with λ. This has the correct sign, and so the phases determined from (29) should be correct and—if necessary at all— the sign of φ_λ in equation (26) has been confirmed.

The phases determined with MIDI on the VLTI are not fully complete, with the constant and linear terms set to zero. But they allow e.g. to break the ambiguity of where the companion in a binary is located with respect to its primary. This property of the MIDI data is needed and used in the discussion of the close binary T Tau S.

We wanted to check the signs of phase derived above from "first principles" with an object where we assume we know the position of the companion. The close binary Z CMa, with separation of $0.1''$, consists of an infrared companion and an FU Ori component. At 4 μm the infrared companion is brighter by a factor of 6.4, this ratio rising with wavelength. The ratio of correlated fluxes at 10 μm, determined is in the range 5–10. We conclude that with these clear inequalities the component much brighter at 4 μm will also be the much brighter component at 10 μm and that it also will show the larger correlated flux. We reject alternative numerically possible relations like a no longer rising flux ratio for $\lambda > 4$ μm with a visibility of the infrared companion at 10 μm 30–60 times smaller than that of the FU Ori component. Z CMa then can be used for calibrating the sign of the phase relation, and we did so with the result that the relations derived here appear correct.

II. IMAGING INFORMATION ENCODED IN MIDI FITS FILES

A. Where is North in the VLTI beams?

The calculation of the field rotation angles φ in the beams that propagate into the Western direction in the VLTI laboratory according to formulas found in [9] or [20, §3.2.5.1] can be done with the shell script `mioFieldAng` which is available from
`http://www.strw.leidenuniv.nl/~mathar/progs/mioFieldAng`. For the case of UTs used—as usual— with beam compressor, this results in

$$\phi = p - a - A + 167.02^\circ \tag{31}$$

where p is the parallactic angle (App. D), A the azimuth as given in the MIDI FITS header, and a the elevation of the object. (This equation is adapted from [20, (Tab 3-3)]; the sign of A is flipped to transform the azimuth conventions

[8].) `mioFieldAng` also calculates ϕ for the ATs. Note that the results may be incorrect if

- The ATs field rotator angle is non-zero,
- ATs are equipped with the star separator (year 2007 and later),
- beams are passing by the PRIMA differential delay lines (year 2007 and later)

This information is presumably correct for all VLTI instruments with the exception of anything parked on the Visitor's Instrument Table.

B. Where is North on the MIDI detector?

The result of an image tracing of the coordinates mentioned in the previous section through the MIDI feeding mirrors and cold optics looks as in Fig. 3 [13] (images are not to scale).

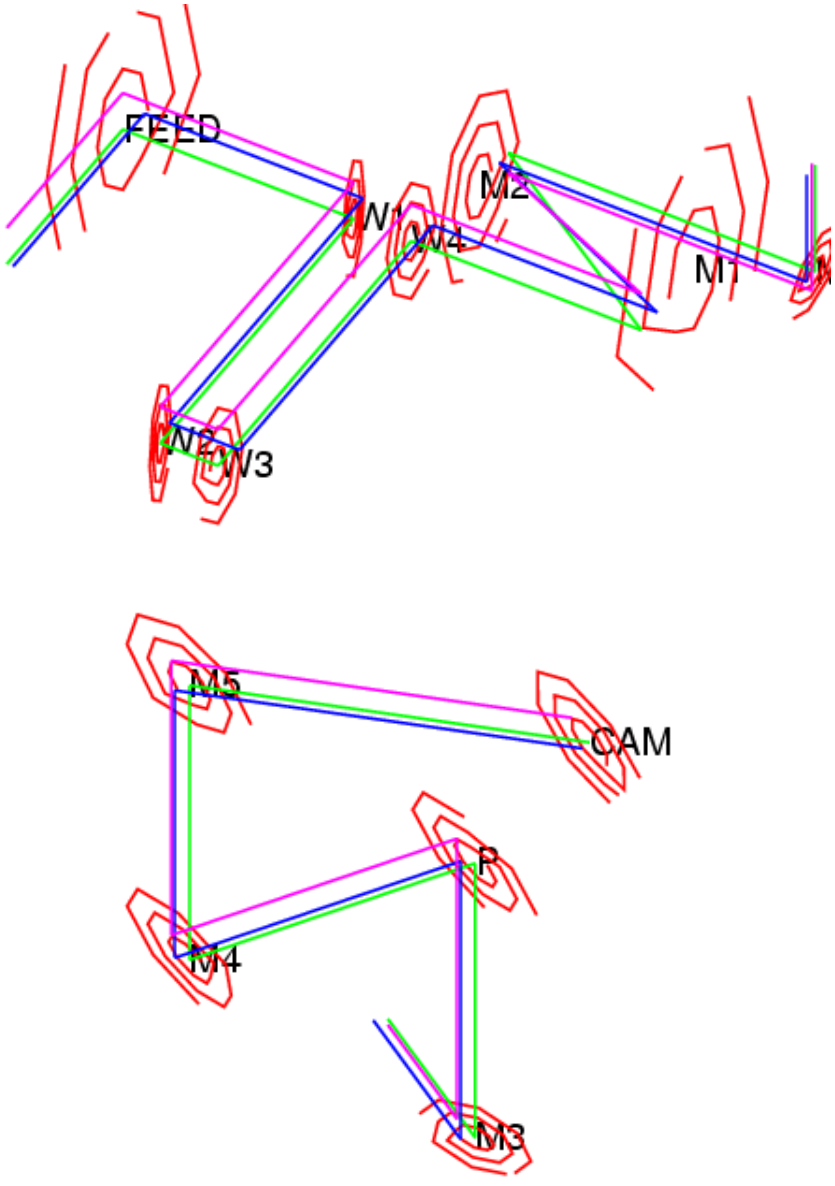

FIG. 3:

In the two graphs above for the photometric channel of beam B, the green line approaches the MIDI feeding optics on the optical axis, the blue line is shifted a little into the +V direction (displaced to the North) and the purple line

is shifted a little into the +W direction (displaced to the ceiling). These are reflected by the feeding optics and pass by the internal delay line of the warm optics, here labeled W1 to W4, with no net rotational effect. (W2 and W3 are piezo-driven.) They move on to M1 to M3 in the cold optics with the intermediate focus between M1 and M2. The second graph shows one arm of the photometric beams coupled out with the mirror named P, reflected by M4 and M5, and approaching the camera CAM, equivalent to the P_B channel in [10, Fig. 10]. Removing P and M4 as to represent the interferometric channels would have no net rotational effect, as comparison of the footprints of the beams that leave M3 and of the beams that leave M4 shows. After the switchyard, before the feeding optics, the blue ray was to the right and the purple ray above the green one—always as seen into the direction of light propagation. Before the camera, the blue line is below and the purple ray to the left of the green one. The camera lens inverts this when it creates the image, which leads to summary in Fig. 4 for both interferometric beams I_1, I_2, and both photometric beams P_A and P_B:

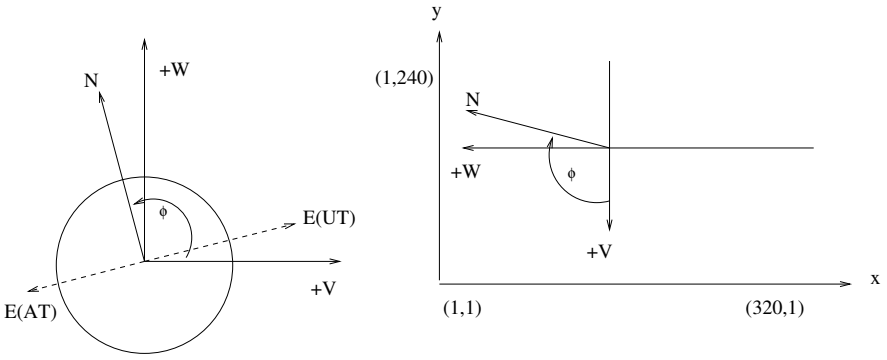

FIG. 4:

In the left diagram, we show the field angle ϕ in a coordinate system as if one was looking from the switchyard to the instruments and feeding optics in the VLTI lab, into the $-U$ direction, as defined in [9]. Note

- this diagram shows an image of the sky directions as if one had inserted a virtual single lens at some U coordinate which created the image on a sheet of paper in the (V, W) plane [7].
- The angle is *not* the same as values for the `ROTATION` column of the `IMAGING_DATA` tables defined in [3].

This ϕ would be obtained from the procedure of Section II A. On the right, the equivalent angle is shown on the MIDI infrared detector from the point of view of the incoming light, looking towards the detector with the beam combiner behind the back. The summary is that the detector watched from the front side (not from the mounting side) or one of the FITS images in the `DATA`i columns of the `IMAGING_DATA` table shows a true image for UTs as one would display a field on the sky, although rotated.

C. How does the baseline project onto the sky?

An overview on the relevant geometry is given in Figure 5 which shows the celestial sphere centered on Paranal and seen from outside—a truly classical perspective.

In Figure 5 A_{Tel1} and A_{Tel2} are the "azimuth" of the telescopes defining the baseline. They can be obtained from the angle τ tabulated in Appendix A, which is an azimuth counted north over east. Seen from the mid-point of the baseline, telescope 1 then is at azimuth τ, telescope 2 at azimuth $A_b = \tau + 180°$, see Fig. 1 above. Let the object be at azimuth A (hierarchical keyword `ESO ISS AZ` referring to the start of measurement) and elevation a (hierarchical header keyword `ESO ISS ALT` referring to the start of measurement).

The projection of the baseline occurs in a plane including the object and the baseline and thus defining the great circle sketched in Figure 5. If θ is the angle on the sky between the object and the point on the horizon with azimuth A_{Tel2}, then the length P of the projected baseline is given by (15), where θ is calculated from the cosine relation,

$$\cos\theta = \cos(A_b - A)\cos\, a. \tag{32}$$

Note:

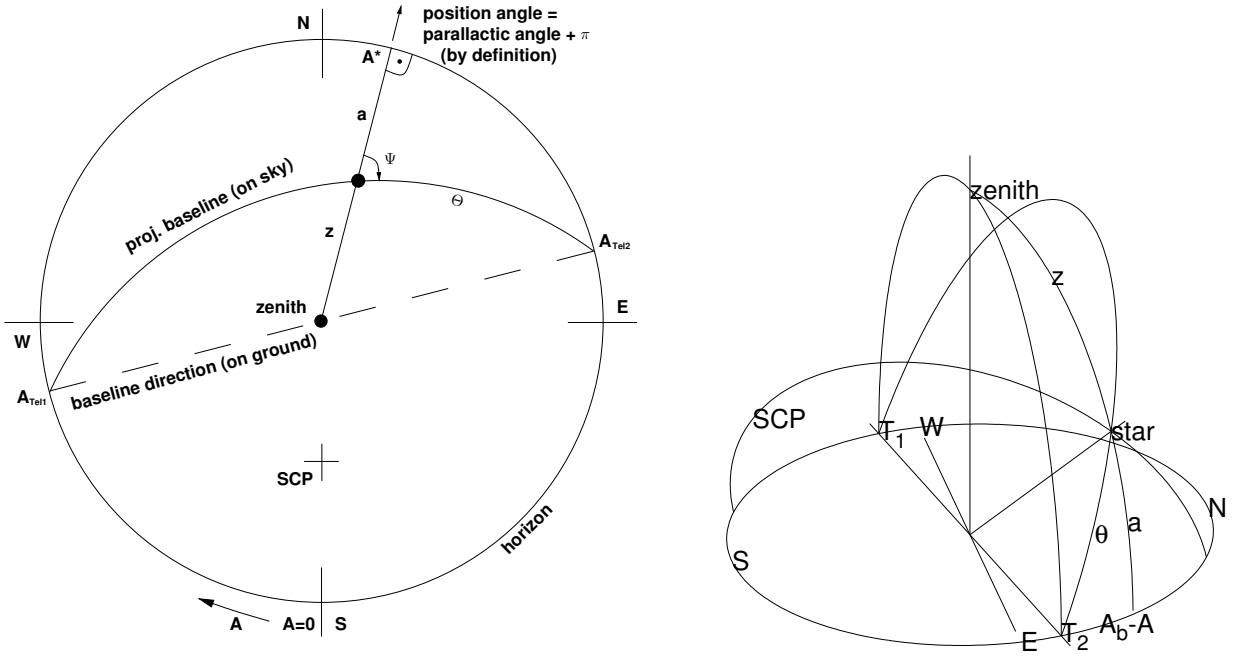

FIG. 5: Celestial sphere over Paranal, seen from the outside. At the left, a projection on the platform: the object is represented by the black dot a zenith distance z from the zenith and elevation $a = 90^\circ - z$ above the horizon. At the right, a perspective view: the north direction through the object is given by the great circle passing through the south celestial pole SCP and the object. The angle θ gives the shortening of the projected baseline, from the angle ψ we have the position angle of the projected baseline on the sky.

- This equation is not strictly compatible to (12) because (32) assumes that the baseline vector points to the horizon, equivalent to a vanishing last component in (12); see Fig. 2 in [14]. If the center of coordinates is moved to the mid-point of the baseline, the unit vector along the baseline becomes

$$\mathbf{T} \equiv \begin{pmatrix} -\cos A_b \\ \sin A_b \\ 0 \end{pmatrix}, \tag{33}$$

  using $z = 90^\circ$ in (13).

As mentioned in (14), $0 \le \theta \le 180^\circ$, which means that Eq. (15) is valid for all quadrants. Following from (15), $\sin\theta$ is the value of the header keyword `ESO ISS PBL12 START` divided by the value of b taken from baselinedata.txt. With this auxiliary quantity, there are various ways of obtaining the position angle p_i of the projected baseline on the sky:

1. (contributed by C Leinert) This is a simplified description, not starting from the basic parameters α, δ, siderial time—as the algorithm in SimVLTI and the algorithm `baseline.pro` in MIA+EWS do— but using the parallactic angle p straight away as available in the primary header keyword `ESO ISS PARANG`. It has the advantage of allowing a quick and easy orientation. The position angle of the projected baseline on the sky p_i follows from the angle ψ as

$$p_i = p + 180^\circ + \psi, \tag{34}$$

   where p is the parallactic angle, the position angle of the upgoing vertical or angle between lines of constant A and constant h. In Fig. 6, p_i is the positional angle of the baseline foot point T_2. ψ is computed from the sine and cosine relations [1, §4.3.149][21, §1.5, 1.6]

$$\frac{\sin\psi}{\sin(A_b - A)} = \frac{1}{\sin\theta}, \tag{35}$$

$$\cos\psi = \frac{\cos(A_b - A) - \cos a \cos\theta}{\sin\theta \sin a} = \frac{\cos(A_b - A)\sin a}{\sin\theta}. \tag{36}$$

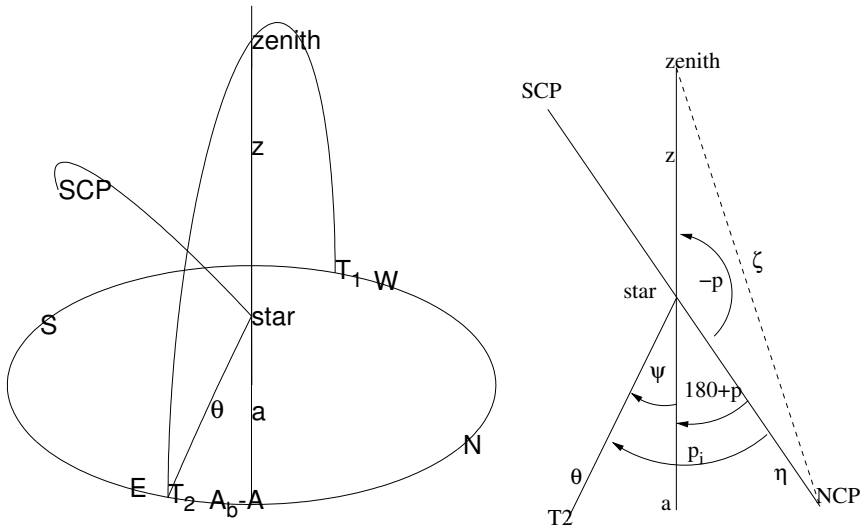

FIG. 6: If we rotate the right part of Fig. 5 until the star and the baseline mid-point merge, and erase some lines, the angles $180^\circ + p$, ψ of Eq. 34 gather around the star as shown. With the standard North-through-East convention of the parallactic angle p, $p < 0$ or $p > 180^\circ$ in this example. In the right picture, the 2D projection centered at the star is seen from the outside of the celestial sphere. Then, looking from the star to the NCP, East is to the right, which appears to the left on the printed paper since the NCP is printed below the star.

When the star crosses the "baseline meridian" defined by the baseline vector **b** shown in Fig. 1, the value of $A_b - A$ is 0 or $\pm 180^\circ, \pm 360^\circ \ldots$; then the $\sin(A_b - A)$ in Eq. (35) switches sign, and the sign of ψ follows. Obviously, the convention chosen in (35) is that ψ increases if the projected baseline vector is more to the East of the NCP—in accordance with the sign convention of the parallactic angle. The principal value of the inverse sine in Eq. (35) then gives ψ in the range $-90^\circ \leq \psi \leq 90^\circ$, i.e., the correct sign with some ambiguity in modulus between $\mid \psi \mid$ and $\mid 180^\circ - \psi \mid$ remaining. This ambiguity is resolved using Eq. (36) which gives $\mid \psi \mid$ in the range 0–180°. (Many programming languages have 2-parameter `atan2` functions to eliminate this problem, and one may skip the calculation of $\sin\theta > 0$ altogether. The alternative is not to calculate p_i and ψ directly, but moving $\cos p_i = -\cos p \cos\psi + \sin p \sin\psi$ and $\sin p_i = -\sin p \cos\psi - \cos p \sin\psi$ into the `atan2` to derive p_i.) The resulting position angle for the projected baseline may be compared with the output of the routine `baseline.pro` under MIA+EWS (which may have been calculated for a different time than the start of the measurement, however). The angles p_i or ψ are not given in the primary header of the MIDI data `*.fits` files.

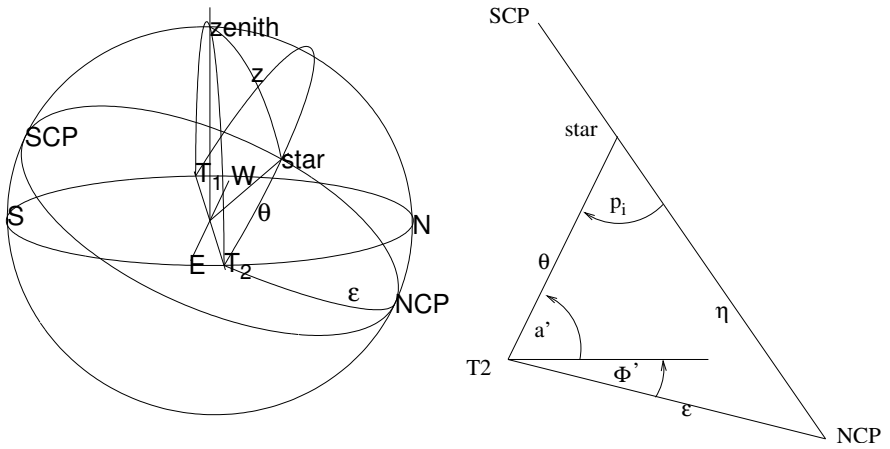

FIG. 7: A derivation of the projected baseline position angle p_i which uses the auxiliary angles a' and Φ' as an alternative to the auxiliary angles ψ and $180^\circ + p$ of Figures 5 and 6.

2. The spherical triangle with the corners at the star, the point T_2 and the NCP shows p_i below the star (Fig. 7). The side lengths in this triangle are θ, η as described in App. D, and ϵ. The dot product between the vector $\mathbf{T}$ to T_2 and the vector $\mathbf{s}_+$ of (D1) to the NCP yields

$$\cos\epsilon = \mathbf{T}\cdot\mathbf{s}_+ = -\cos\Phi\cos A_b. \tag{37}$$

The cosine formula of spherical trigonometry provides

$$\cos\epsilon = \cos\theta\cos\eta + \sin\theta\sin\eta\cos p_i, \tag{38}$$

$$\Rightarrow \cos p_i = -\frac{\cos\Phi\cos A_b + \cos\theta\sin\delta}{\sin\theta\cos\delta}. \tag{39}$$

The associated sine formula is

$$\frac{\sin p_i}{\sin\epsilon} = \frac{\sin(a'+\Phi')}{\sin\eta}, \tag{40}$$

where $a'+\Phi'$ is the sum of the two angles subtended at T_2. a' is the inclination of the projected baseline towards the horizontal. It can be derived from the z-component of the cross product $\mathbf{T}\times\mathbf{s}$ with (22) and (33),

$$\cos a' = -\frac{\cos A_b\cos\delta\sin h + \sin A_b\left[\cos\Phi\sin\delta - \sin\Phi\cos\delta\cos h\right]}{\sin\theta};\quad 0\le a'\le\pi, \tag{41}$$

or by using "formula C" [21, §1.7]

$$\cos a' = \frac{\cos a\sin(A_b - A)}{\sin\theta}. \tag{42}$$

The simpler sine formula

$$\frac{\sin a'}{\sin a} = \frac{1}{\sin\theta} \tag{43}$$

has the disadvantage of not solving the ambiguity $a' \leftrightarrow \pi - a'$. [The associated $\cos a' = \sin\psi\cos a$ and $\sin a'/\sin a = \sin\psi/\sin(A_b - A)$ are probably not of much value beyond a check.] Φ' is the inclination of the plane that contains the telescopes and the NCP towards the horizontal. Φ' is found by looking at the zenith component of the cross product $\mathbf{T}\times\mathbf{s}_+$ (which is perpendicular to the plane),

$$\cos\Phi' = -\frac{\sin A_b\cos\Phi}{|\sin\epsilon|}. \tag{44}$$

3. One may also use the vector algebraic method to span a tangential plane across the celestial sphere touching it at the position of the star, and compute the two 2D directions in this plane towards the NCP on one hand and towards the T_2 on the other. This method is the least ambiguous w.r.t. signs. The tangential plane is given by two unit vectors perpendicular to $\mathbf{s}$ of (22). They are rather arbitrarily chosen to point along $\partial\mathbf{s}/\partial h$ and $\partial\mathbf{s}/\partial\delta$; their relation to the equatorial system will lead to a simple expansion further down:

$$\mathbf{e}_h = \begin{pmatrix} \sin\Phi\sin h \\ \cos h \\ -\cos\Phi\sin h \end{pmatrix};\quad \mathbf{e}_\delta = \begin{pmatrix} \cos\Phi\cos\delta + \sin\Phi\sin\delta\cos h \\ -\sin\delta\sin h \\ \sin\Phi\cos\delta - \cos\Phi\sin\delta\cos h, \end{pmatrix}, \tag{45}$$

such that

$$\mathbf{s}\cdot\mathbf{e}_h = \mathbf{s}\cdot\mathbf{e}_\delta = \mathbf{e}_1\cdot\mathbf{e}_\delta = 0;\quad |\mathbf{e}_h| = |\mathbf{e}_\delta| = 1;\quad \mathbf{s}\times\mathbf{e}_\delta = \mathbf{e}_h. \tag{46}$$

The decomposition of the direction to the NCP (D1) perpendicular to and parallel to this plane defines three expansion coefficients $c_{1,2,3}$,

$$\mathbf{s}_+ = c_1\mathbf{s} + c_2\mathbf{e}_h + c_3\mathbf{e}_\delta. \tag{47}$$

Multiplying this equation in turn with $\mathbf{e}_h$ and $\mathbf{e}_\delta$ yields

$$c_2 = 0;\quad c_3 = \mathbf{s}_+\cdot\mathbf{e}_\delta = \cos\delta. \tag{48}$$

(Obviously, moving the star towards the NCP induces no change in the h, only in the δ coordinate.) The direction to T_2 is projected into the same tangential plane, defining three expansion coefficients $c'_{1,2,3}$,

$$\mathbf{T} = c'_1\mathbf{s} + c'_2\mathbf{e}_h + c'_3\mathbf{e}_\delta. \tag{49}$$

Building the dot product of this equation with $\mathbf{e}_h$ using (33) yields

$$c'_2 = -\cos A_b \sin\Phi \sin h + \sin A_b \cos h, \tag{50}$$

and building the dot product of (49) with $\mathbf{e}_\delta$ yields

$$c'_3 = -\cos A_b \cos\Phi \cos\delta - \cos A_b \sin\Phi \sin\delta \cos h - \sin A_b \sin\delta \sin h, \tag{51}$$

where we replace

$$\sin\Phi\cos h \rightarrow \frac{\cos\Phi\sin\delta + \cos A \sin z}{\cos\delta} \tag{52}$$

in the second term—which follows from equating the first components in (13) and (22)— and where we replace

$$\sin h \rightarrow \frac{\sin A \sin z}{\cos\delta} \tag{53}$$

in the last term—which follows from equation the second components in (13) and (22). Further standard trigonometric transformations [1, 4.3.10,4.3.17] produce, with (32),

$$c'_3 = \frac{-\cos A_b\cos\Phi - \cos(A_b - A)\sin z\sin\delta}{\cos\delta} = -\frac{\cos A_b\cos\Phi + \cos\theta\sin\delta}{\cos\delta}. \tag{54}$$

p_i is the angle that that rotates the vector (c_2, c_3) within the tangent plane into the direction (c'_2, c'_3). Eq. (48) shows that $\mathbf{e}_\delta$ is the direction from the star to the NCP. From the orientation of the axes shown in (46) we conclude that components along $\mathbf{e}_h$ are pointing West (inheriting the sign convention from the hour angle). From the similarity between (54) and (39), we may eventually compute

$$\cos p_i = c'_3/\sin\theta; \quad \sin p_i = -c'_2/\sin\theta. \tag{55}$$

More variations on the theme like a formulation with Euler angles [5][11, App. 1] may exist.

OIFITS [18] defines an x-axis pointing to the East and a y-axis pointing to the North, but no associated angle. Our convention implies $x \propto \sin p_i$ and $y \propto \cos p_i$ which is different from the Calabretta-Greisen azimuth convention, Fig. 3 and formulas (12)–(13) in [5], who start at an angle of zero along the negative y-axis.

Quick interactive ways to obtain p_i are

- to start the Java applet `http://www.strw.leidenuniv.nl/~mathar/prima/prErrWeb.html`, select the two stations, insert the star coordinates at `PS: RA` and `PS: DEC`, the sidereal time labeled `LST` and click on `Update below!`.
- or to start the Java applet `http://obswww.unige.ch/~segransa/apes/protoapes/Welcome.html`, select baselines and star coordinates, and read off the value of `Theta`.
- The values of A_b and p_i are also reported by recent versions of `http://www.strw.leidenuniv.nl/~mathar/progs/mioFieldAng`, which scans the FITS files of an entire UNIX directory.

Programmers would probably use the `SLA_DBEAR` function of the SLALIB. Remark:

- Since approximately June 2005, ISS adds two keywords `ESO ISS PBLA12 START` and `END` to the primary FITS headers, which are *not* directly related to θ or p_i. These header keywords are derived from the projected baseline vector $\mathbf{P}$. If $\mathbf{P}$ is projected onto the (U, V) plane of the Paranal platform, the azimuth angle of this horizontal, doubly projected vector angle is reported in `ESO ISS PBLA12`, modulo 180°. At small delay D, the direction of $\mathbf{P}$ becomes parallel to $\mathbf{b}$ and the value of this keyword approaches τ or $\tau \pm 180°$. The major difference between this implementation and the one formulated above is that the formulation of this script here is compatible with the OIFITS standard [18, App A] which explicitly defines the plane for the visibility calculation to be normal to the direction of the phase center. A change request has been issued as SPR VLTSW20060066, see App. G 2.

APPENDIX A: BASELINE AZIMUTH ANGLES

This section tabulates the baseline orientation τ from T_1 to T_2 in the notation of `http://www.eso.org/observing/etc/doc/vlti/baseline/baselinedata.txt`, which means the angle is zero if T_2 is north of T_1, and $+90°$ if it is East of T_1: Fig. 1. (Note that the tables in [6] use a different definition.) These angles are updated from App. G 1 and typically differ from those of the web page in the last two digits provided. (A corresponding change request has been issued, see App. H.)

The values are calculated as follows from geographical coordinates (λ_1, Φ_1) and (λ_2, Φ_2): We construct the great circle around the Earth center that connects T_1 and T_2, where

$$\mathbf{T}_i \equiv \rho \begin{pmatrix} \sin\lambda_i \cos\Phi_i \\ \cos\lambda_i \cos\Phi_i \\ \sin\Phi_i \end{pmatrix}, \quad i = 1, 2 \tag{A1}$$

are the telescope coordinates in a geocentric system. The surface normal to this circle is $\hat{\mathbf{J}} \equiv \frac{1}{\rho^2 \sin Z} \mathbf{T}_1 \times \mathbf{T}_2$. Rotation around this axis by the angle Z of Sec. (I G) moves $\mathbf{T}_1$ onto $\mathbf{T}_2$. Imagine the tangent plane touching the Earth sphere at $\mathbf{T}_1$. At this point, the unit vector to the geographic North direction along the tangent plane is

$$\hat{\mathbf{N}}_1 \equiv \begin{pmatrix} -\sin\lambda_1 \sin\Phi_1 \\ -\cos\lambda_1 \sin\Phi_1 \\ \cos\Phi_1 \end{pmatrix} \sim \partial\mathbf{T}_1/\partial\Phi_1; \quad |\hat{\mathbf{N}}_1| = 1. \tag{A2}$$

The unit vector to the East at the same point is

$$\hat{\mathbf{E}}_1 \equiv \begin{pmatrix} \cos\lambda_1 \\ -\sin\lambda_1 \\ 0 \end{pmatrix} \sim \partial\mathbf{T}_1/\partial\lambda_1; \quad |\hat{\mathbf{E}}_1| = 1. \tag{A3}$$

At this point, the unit vector along the great circle into the direction of $\mathbf{T}_2$ is $\hat{\mathbf{J}} \times \frac{1}{\rho}\mathbf{T}_1$. τ is identified by its decomposition $\hat{\mathbf{J}} \times \frac{1}{\rho}\mathbf{T}_1 = \cos\tau\hat{\mathbf{N}}_1 + \sin\tau\hat{\mathbf{E}}_1$ within the tangent plane:

$$\cos\tau = \frac{\cos\Phi_1 \sin\Phi_2 - \sin\Phi_1 \cos\Phi_2 \cos(\lambda_1 - \lambda_2)}{\sin Z}; \quad \sin\tau = -\frac{\cos\Phi_2 \sin(\lambda_1 - \lambda_2)}{\sin Z}. \tag{A4}$$

Note that, strictly speaking, τ does not transform into $\tau \pm 180°$ if the roles of $\mathbf{T}_1$ and $\mathbf{T}_2$ are swapped, because the great circles that fixate the τ in the two tangent planes at either telescope are not loxodromes. Within the milli-degree precision of tables I–III, this is not of concern, which means that the table appears to be "antisymmetric" along its diagonal in this sense of $\tau \leftrightarrow \tau \pm 180°$ if $T_1 \leftrightarrow T_2$.

	A0	A1	B0	B1	B2	B3	B4	B5	C0	C1	C2
A0			71.007	134.456	142.583	146.980	149.705	151.552	71.014	116.016	127.325
A1			7.581	71.020	116.010	134.443	142.573	146.971	26.020	71.020	97.579
B0	-108.993	-172.419							71.020	134.442	142.573
B1	-45.545	-108.980							7.581	71.020	116.010
B2	-37.417	-63.990							-0.552	26.020	71.020
B3	-33.020	-45.558							-4.951	7.581	26.020
B4	-30.295	-37.428							-7.678	-0.552	7.581
B5	-28.448	-33.029							-9.526	-4.951	-0.552
C0	-108.986	-153.980	-108.980	-172.419	179.448	175.049	172.322	170.474			
C1	-63.984	-108.980	-45.558	-108.980	-153.980	-172.419	179.448	175.049			
C2	-52.675	-82.421	-37.428	-63.990	-108.980	-153.980	-172.419	179.448			
C3	-45.551	-63.990	-33.029	-45.558	-63.990	-108.980	-153.980	-172.419			
D0	-108.983	-135.543	-108.980	-142.668	-153.980	-162.112	-168.020	-172.419	-108.980	-153.980	-165.293
D1	-63.984	-82.420	-55.857	-75.295	-90.549	-108.984	-127.421	-142.678	-45.551	-63.984	-82.418
D2	-52.675	-63.987	-45.553	-55.857	-63.986	-75.295	-90.549	-108.984	-37.422	-45.551	-52.675
E0	-108.991	-127.422	-108.991	-130.791	-139.952	-147.648	-153.988	-159.183	-108.994	-135.557	-145.861
G0	-108.989	-123.022	-108.988	-124.932	-132.184	-138.731	-144.523	-149.587	-108.989	-127.422	-135.552
G1	-63.986	-72.116	-60.173	-68.385	-73.448	-79.240	-85.786	-93.038	-55.857	-63.986	-69.180
G2	-129.544	-140.990	-132.184	-144.523	-149.587	-153.986	-157.800	-161.111	-135.552	-148.792	-153.987
H0	-108.987	-118.447	-108.986	-119.290	-124.240	-128.968	-133.429	-137.596	-108.987	-120.296	-125.685
I1	-87.947	-95.989	-86.365	-94.947	-99.521	-104.220	-108.983	-113.747	-84.541	-93.729	-98.679
J1	-97.677	-105.172	-96.892	-104.900	-108.986	-113.071	-117.116	-121.080	-95.992	-104.588	-108.986
J2	-87.183	-94.052	-85.786	-93.038	-96.889	-100.853	-104.897	-108.983	-84.210	-91.881	-95.989
J3	-134.002	-139.947	-135.549	-141.719	-144.522	-147.142	-149.586	-151.864	-137.285	-143.680	-146.553
J4	-139.949	-145.237	-141.719	-147.141	-149.585	-151.863	-153.984	-155.959	-143.679	-149.220	-151.694
J5	-147.645	-152.009	-149.585	-153.984	-155.959	-157.798	-159.512	-161.110	-151.694	-156.106	-158.070
J6	-153.986	-157.560	-155.959	-159.512	-161.110	-162.600	-163.993	-165.295	-158.070	-161.580	-163.147
K0	-108.986	-116.110	-108.985	-116.580	-120.295	-123.916	-127.420	-130.786	-108.986	-117.116	-121.080
L0	-108.986	-115.694	-108.985	-116.110	-119.604	-123.021	-126.339	-129.541	-108.985	-116.580	-120.295
M0	-108.985	-115.324	-108.985	-115.694	-118.992	-122.225	-125.374	-128.424	-108.985	-116.110	-119.604
U1	-172.421	179.455	175.060	170.482	169.148	168.142	167.356	166.726	161.023	161.018	161.017
U2	-161.111	-166.513	-165.294	-170.374	-172.420	-174.210	-175.787	-177.184	-169.930	-174.541	-176.366
U3	-153.985	-158.382	-156.472	-160.826	-162.730	-164.475	-166.079	-167.555	-159.178	-163.446	-165.294
U4	-130.236	-135.549	-131.365	-136.882	-139.450	-141.890	-144.202	-146.390	-132.614	-138.342	-140.990

TABLE I: Baseline orientation angles τ (degrees) obtained from App. G 1. T_2 is an AT on the A to C rails.

	C3	D0	D1	D2	E0	G0	G1	G2	H0	I1	J1
A0	134.449	71.017	116.016	127.325	71.009	71.012	116.015	50.456	71.014	92.054	82.324
A1	116.010	44.457	97.580	116.013	52.578	56.979	107.884	39.010	61.553	84.011	74.829
B0	146.971	71.020	124.143	134.447	71.009	71.012	119.827	47.816	71.014	93.636	83.109
B1	134.443	37.332	104.705	124.143	49.210	55.069	111.615	35.477	60.710	85.053	75.100
B2	116.010	26.020	89.451	116.014	40.048	47.816	106.552	30.413	55.760	80.479	71.015
B3	71.020	17.888	71.016	104.705	32.352	41.270	100.760	26.014	51.032	75.781	66.929
B4	26.020	11.981	52.579	89.451	26.012	35.477	94.215	22.200	46.571	71.017	62.885
B5	7.581	7.581	37.322	71.016	20.817	30.413	86.962	18.889	42.404	66.253	58.920
C0		71.020	134.449	142.578	71.006	71.011	124.143	44.448	71.014	95.460	84.008
C1		26.020	116.016	134.449	44.443	52.578	116.014	31.208	59.704	86.272	75.413
C2		14.708	97.582	127.325	34.139	44.448	110.820	26.013	54.315	81.322	71.014
C3		7.581	71.014	116.016	26.010	37.323	104.705	21.614	49.213	76.211	66.616
D0	-172.419				70.992	71.006	134.449	34.139	71.012	100.070	86.268
D1	-108.986				7.579	26.016	116.013	10.760	44.450	77.357	65.820
D2	-63.984				-0.551	14.706	97.580	4.977	34.145	64.677	55.760
E0	-153.990	-109.008	-172.421	179.449		71.020	146.979	14.708	71.018	106.558	89.451
G0	-142.677	-108.994	-153.984	-165.294	-108.980				71.017	116.021	94.215
G1	-75.295	-45.551	-63.987	-82.420	-33.021				7.580	40.053	35.477
G2	-158.386	-145.861	-169.240	-175.023	-165.292				107.884	129.012	111.615
H0	-130.787	-108.989	-135.550	-145.855	-108.982	-108.983	-172.420	-72.116		149.709	116.014
I1	-103.789	-79.930	-102.643	-115.323	-73.443	-63.979	-139.947	-50.988	-30.291		26.013
J1	-113.385	-93.733	-114.180	-124.241	-90.549	-85.786	-144.523	-68.385	-63.986	-153.987	
J2	-100.237	-80.374	-98.678	-108.982	-75.292	-68.380	-124.927	-56.859	-45.548	-82.421	
J3	-149.221	-141.457	-153.984	-158.748	-146.857	-153.984	-173.968	-138.727	-175.787	170.478	
J4	-153.984	-148.274	-158.747	-162.730	-153.982	-161.108	-176.603	-149.583	179.453	169.148	
J5	-159.891	-156.475	-164.475	-167.555	-162.113	-168.728	-179.694	-161.108	175.052	167.726	
J6	-164.605	-162.732	-168.916	-171.339	-168.020	-173.968	177.942	-168.728	172.325	166.726	
K0	-124.931	-108.987	-127.420	-135.550	-108.982	-108.983	-153.985	-88.428	-108.983	-168.021	179.448
L0	-123.916	-108.986	-126.087	-133.759	-108.982	-108.983	-150.618	-90.549	-108.982	-160.324	-165.292
M0	-123.021	-108.986	-124.929	-132.182	-108.982	-108.982	-147.644	-92.285	-108.982	-153.983	-153.980
U1	161.016	134.456	146.983	149.707	116.016	104.705	134.452	80.479	92.818	110.308	99.316
U2	-177.948	179.448	174.010	172.325	167.355	154.672	157.648	151.552	131.958	137.817	127.323
U3	-166.979	-165.294	-172.418	-175.021	-172.417	179.452	172.326	-175.019	161.017	157.651	149.706
U4	-143.493	-135.551	-147.141	-151.863	-139.239	-143.975	-165.294	-130.785	-158.381	-176.363	177.716

TABLE II: Baseline orientation angles τ obtained from App. G 1, continued from Table I. T_2 is an AT on the C to J rails.

	J2	J3	J4	J5	J6	K0	L0	M0	U1	U2	U3	U4
A0	92.818	45.998	40.051	32.355	26.015	71.015	71.015	71.015	7.579	18.889	26.016	49.764
A1	85.948	40.053	34.763	27.992	22.440	63.891	64.306	64.676	-0.545	13.488	21.619	44.451
B0	94.214	44.452	38.281	30.415	24.041	71.015	71.015	71.016	-4.940	14.707	23.528	48.636
B1	86.962	38.281	32.859	26.016	20.488	63.421	63.891	64.306	-9.518	9.626	19.174	43.119
B2	83.112	35.479	30.415	24.041	18.891	59.706	60.396	61.008	-10.852	7.580	17.271	40.551
B3	79.147	32.859	28.137	22.202	17.400	56.084	56.980	57.776	-11.858	5.790	15.525	38.111
B4	75.103	30.414	26.016	20.488	16.007	52.580	53.662	54.627	-12.644	4.213	13.922	35.798
B5	71.018	28.137	24.041	18.891	14.705	49.214	50.460	51.576	-13.274	2.816	12.446	33.610
C0	95.791	42.715	36.321	28.307	21.930	71.015	71.015	71.015	-18.977	10.070	20.823	47.386
C1	88.119	36.321	30.780	23.895	18.421	62.885	63.421	63.891	-18.982	5.459	16.554	41.658
C2	84.011	33.447	28.307	21.930	16.853	58.920	59.706	60.396	-18.983	3.634	14.706	39.010
C3	79.763	30.779	26.016	20.109	15.395	55.070	56.084	56.980	-18.984	2.052	13.021	36.507
D0	99.626	38.544	31.726	23.526	17.268	71.014	71.014	71.015	-45.544	-0.552	14.706	44.450
D1	81.322	26.016	21.254	15.525	11.084	52.581	53.913	55.071	-33.017	-5.990	7.582	32.859
D2	71.018	21.252	17.271	12.446	8.661	44.451	46.241	47.818	-30.293	-7.675	4.979	28.137
E0	104.709	33.143	26.019	17.887	11.980	71.018	71.018	71.018	-63.984	-12.645	7.583	40.761
G0	111.620	26.016	18.892	11.272	6.032	71.017	71.018	71.018	-75.295	-25.328	-0.548	36.025
G1	55.074	6.032	3.397	0.306	-2.058	26.015	29.382	32.357	-45.549	-22.352	-7.674	14.706
G2	123.141	41.273	30.417	18.892	11.272	91.572	89.451	87.716	-99.522	-28.448	4.981	49.215
H0	134.452	4.213	-0.547	-4.948	-7.675	71.017	71.018	71.018	-87.183	-48.042	-18.983	21.619
I1	97.579	-9.522	-10.852	-12.274	-13.274	11.979	19.676	26.017	-69.693	-42.183	-22.349	3.637
J1						-0.552	14.708	26.020	-80.684	-52.677	-30.294	-2.284
J2						-9.525	-0.551	7.580	-71.414	-47.058	-28.446	-5.989
J3						152.883	145.067	137.813	-121.978	-94.947	-49.941	71.006
J4						154.679	148.489	142.582	-130.022	-108.987	-63.986	104.705
J5						156.253	151.553	146.979	-140.592	-129.541	-108.984	130.048
J6						157.201	153.420	149.704	-149.221	-145.854	-153.989	140.455
K0	170.475	-27.117	-25.322	-23.747	-22.799		71.020	71.020	-93.039	-63.986	-37.418	-3.036
L0	179.449	-34.933	-31.511	-28.447	-26.580	-108.980		71.020	-94.052	-66.999	-41.603	-10.852
M0	-172.420	-42.187	-37.418	-33.021	-30.296	-108.980	-108.980		-94.948	-69.697	-45.549	-18.983
U1	108.586	58.023	49.979	39.409	30.779	86.962	85.948	85.053		26.015	32.357	60.396
U2	132.942	85.053	71.014	50.459	34.146	116.014	113.001	110.304	-153.985		40.053	81.318
U3	151.554	130.059	116.014	71.016	26.011	142.582	138.397	134.451	-147.643	-139.947		110.820
U4	174.011	-108.994	-75.295	-49.952	-39.545	176.964	169.148	161.017	-119.604	-98.682	-69.180	

TABLE III: Baseline orientation angles τ obtained from App. G 1, continued from Table I and II. T_2 is an UT or an AT on the J to M rails.

APPENDIX B: HEAD FILES OF SPLIT EXPOSURES

Some hints on figuring out which of the files in a directory might be such "head" files of an exposure:

- Exposures are scheduled by the instrument software to start on straight seconds (w/o chopping) or on times commensurable with the chopping period. Since the chopping frequency is often 2 Hz, files with "straight" millisecond identifiers like `MIDI.*.000.fits` and `MIDI.*.250.fits` are usually the first ones of an exposure, whereas those with some random milliseconds like `MIDI.*.376.fits` are the followup files.
- If the keyword value of `ORIGFILE` in the FITS header ends on `_01.fits`, it is such a head file, whereas a higher index like `_02.fits` of the keyword value characterizes followup files.
- If the keyword value of `ESO OCS EXPO FILENO` in the FITS header is 1, it is such a head file. The other files show higher integers $2, 3 \ldots$ with this keyword.

For UNIX directories with the raw MIDI FITS files, the head files can simply be listed by

```
ls -l MIDI.????-??-??T??:??:??.???_01.fits
```

For directories assembled by the ESO pipeline, one might use

```
fitshead MIDI*.fits | egrep '(ORIGFILE|ARCFILE)' | \
awk '{if (NR%2 ==1) n=strtonum(substr($2,31,2)); else if (n==1) print $3}'
```

to list them. A C program `mioFitsFNames.c` that re-links a directory with files named according to the original instrument convention into another directory with the pipeline naming convention is available on the MPIA server.

APPENDIX C: PUPIL ROTATION IN THE VLTI TRAIN

In a color encoding consistent with the one above, the transversal of the beam for a UT pointing to the zenith looks as follows in the overview:

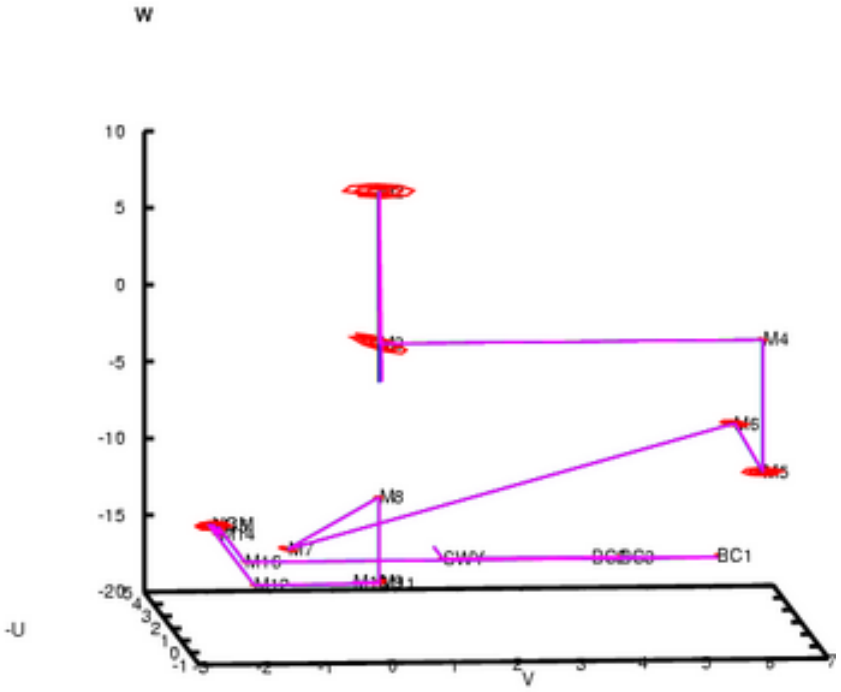

The uppermost mirror is M2, the one below M3; M1 is not shown. A detail of the three mirrors of the beam compressor looks as follows:

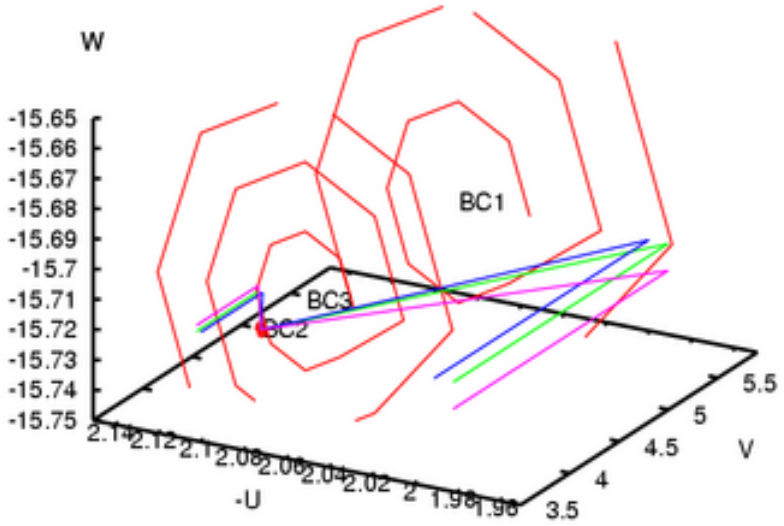

One more horizontal turn by the SWY mirror moves the beam leaving BC3 onto the feeding optics shown in Section II A. Zooming into the M13–M15 of the MDL it looks as follows:

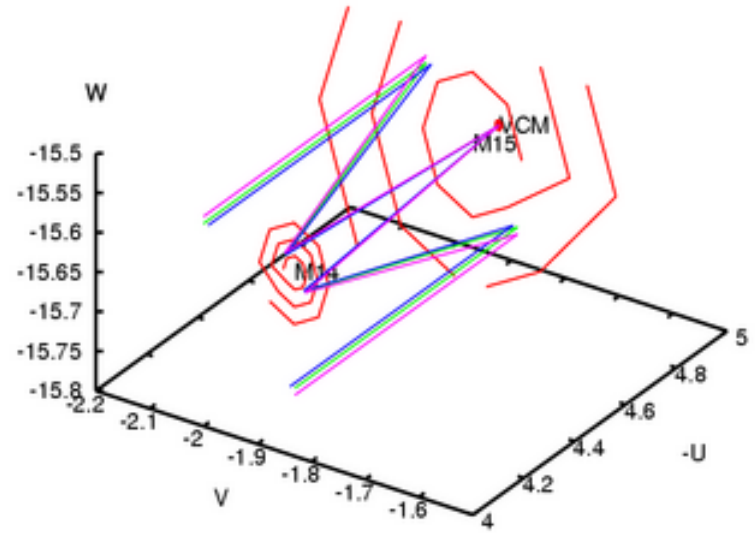

Because the positions of the mirrors of the UT Coudé train are unavailable to the author, and a model of the foci higher up could not be made, we do not follow the rays further back through the optics.

APPENDIX D: PARALLACTIC ANGLE

The coordinates of the NCP and SCP in the topocentric Cartesian coordinate system of Section I H 2 are given by insertion of $\delta = \pm 90°$ into (22),

$$\mathbf{s}_\pm = \pm \begin{pmatrix} \cos\Phi \\ 0 \\ \sin\Phi \end{pmatrix}. \tag{D1}$$

We define the parallactic angle p with the NCP as the reference to tie it to the VLT convention (which traces back to its use of the generic SLALIB).

Building the three dot products between the star direction of (22), between the zenith direction $(0, 0, 1)$ and between $\mathbf{s}_+$ yields the three cosines of their angular separations z, η and ζ in the spherical triangle formed by the star, the

zenith and the NCP in Fig. 6,

$$\cos z = \sin\Phi\sin\delta + \cos\Phi\cos\delta\cos h, \tag{D2}$$
$$\cos\eta = \mathbf{s}_+ \cdot \mathbf{s} = \sin\delta, \tag{D3}$$
$$\cos\zeta = \sin\Phi. \tag{D4}$$

The sine and cosine formula of spherical geometry [1, 4.3.149] yield

$$\frac{\sin p}{\sin\zeta} = \frac{\sin A}{\sin\eta}, \tag{D5}$$
$$\cos\zeta = \cos z\cos\eta + \sin z\sin\eta\cos p. \tag{D6}$$

The sign in (D5) has been chosen to yield $p > 0$ if the zenith is to the East of the NCP from the point of view of the star. (In the right part of Fig. 6, $p < 0$ or $p > 180°$, respectively.) We may solve the first of these equations for $\sin p$ and the second for $\cos p$ and build the quotient

$$\tan p = \frac{\sin A\sin\zeta\sin z}{\cos\zeta - \cos z\cos\eta} \tag{D7}$$

In the numerator we replace $\sin A\sin z \to \cos\delta\sin h$ [from a comparison of the middle components of (13) and (22)]; in the denominator rewrite $\cos\zeta$ with (D4) and $\cos z\cos\eta$ with the product of (D2) and (D3), replace $1-\sin^2\delta \to \cos^2\delta$ in the denominator and $\sin\zeta \to \cos\Phi$ from (D4) in the numerator,

$$\begin{aligned}\tan p &= \frac{\sin\zeta\cos\delta\sin h}{\sin\Phi - (\sin\Phi\sin^2\delta + \cos\Phi\cos\delta\sin\delta\cos h)} = \frac{\sin\zeta\cos\delta\sin h}{\sin\Phi\cos^2\delta - \cos\Phi\cos\delta\sin\delta\cos h} \\ &= \frac{\sin\zeta\sin h}{\sin\Phi\cos\delta - \cos\Phi\sin\delta\cos h} = \frac{\sin h}{\tan\Phi\cos\delta - \sin\delta\cos h},\end{aligned} \tag{D8}$$

as found in Section 3.2.2 of the older version of [20].

APPENDIX E: SNAPSHOTS OF PRIMA DOCUMENTATION

To make equation (19) more plausible, two related pages of the PRIMA error budget [23] are reproduced here. The full text is available from `http://www.strw.leidenuniv.nl/~mathar/public/mathar15753-0001.pdf`. Appendices E and F use an azimuth convention "North-through-West."

28.3.5 Tangential Approximation

The expansion of (52) in Δz and ΔA reads

$$C \equiv \cos\tau - 1 = -\frac{1}{2}\left[(\Delta z)^2 + \sin^2\bar{z}(\Delta A)^2\right] + \frac{1}{24}\left[(\Delta z)^4 + 3(\Delta z)^2(\Delta A)^2 + \sin^2\bar{z}(\Delta A)^4\right] + \cdots \quad (46)$$

The inversion of the power series of the cosine

$$C = -\frac{1}{2}\tau^2 + \frac{1}{24}\tau^4 - \frac{1}{6!}\tau^6 + \cdots \quad (47)$$

yields [1, 3.6.25]

$$\tau^2 = -2C + \frac{1}{3}C^2 - \frac{4}{45}C^3 + \frac{1}{35}C^4 + \ldots \quad (48)$$

Insertion of C from above yields the terms in (54) up to mixed 4th order in Δz and ΔA:

$$\tau^2 = (\Delta z)^2 + \sin^2\bar{z}(\Delta A)^2 - \frac{1+2\cos^2\bar{z}}{12}(\Delta z)^2(\Delta A)^2 - \frac{1}{12}\cos^2\bar{z}\sin^2\bar{z}(\Delta A)^4 + \cdots \quad (49)$$

Δz and ΔA are limited to the PRIMA FOV of $2'$, which means the relative change in τ^2 introduced by the two 4th order terms is limited to roughly a fourth of $(\Delta z)^2, (\Delta A)^2 < 3.4\cdot 10^{-7}$ rad^2. The relative correction in τ is limited to half of this, $4\cdot 10^{-8}$ rad. Since τ is also less than $2' = 120''$, the absolute contribution of the 4th order terms to τ is never larger than 5 μas. In this sense, Equation (56) does not suffer from distortions as it ignores wrapping effects in the coordinate system.

The equivalent extension of (55) to mixed third order is

$$\begin{aligned}\frac{\Delta D}{b} \;\approx\;& \sin\bar{A}\sin\bar{z}\Delta A - \cos\bar{A}\cos\bar{z}\Delta z \\ &+\frac{1}{24}\cos\bar{A}\cos\bar{z}(\Delta z)^3 - \frac{1}{8}\sin\bar{A}\sin\bar{z}(\Delta z)^2\Delta A - \frac{1}{24}\sin\bar{A}\sin\bar{z}(\Delta A)^3 + \frac{1}{8}\cos\bar{A}\cos\bar{z}\Delta z(\Delta A)^2\end{aligned}$$

Taking into account the coefficients, the relative change by the third order terms is limited to a sixth of $(\Delta z)^2, (\Delta A)^2 < 3.4\cdot 10^{-7}$. This correction obviously is of the same order as the relative correction to τ, since both parameters are tightly linked by Equation (57).

28.4 Impact on astrometry

The sidereal motion of the two stars limits the time over which one can naïvely calculate the DOPD as a simple mean over an observation period, for example during a data compression step in the DRS. The DOPD is a sinusoidal function of time as shown in Fig. 43. The maximum amplitude X_m is 0.117 m if the longest baseline $b = 202$ m is used at the maximum star separation $\tau = 2'$. (The longest baseline admitted in [53] is 145 m.) Assigning the mean OPD to the middle of an observation period is exact for strictly linear motion in t, $\Delta D(t) = \Delta D(t_0) + \frac{\partial\Delta D(t)}{\partial t}(t - t_0)$. The DOPD velocity may reach up to $\partial\Delta D(t)/\partial t \le X_m\omega_L \approx 8.5$ μm/s, where $\omega_L = 2\pi/(24\cdot 3600)$ 1/s$\approx 7.3\cdot 10^{-5}$ 1/s is the angular velocity. The error results from higher order derivatives, here the second order derivative $\partial^2\Delta D(t)/\partial t^2 \le X_m\omega_L^2$. In such 2nd order approximation, the difference between the true mean (the integral over the interval divided by the length of the interval) and the actual value in the middle of the interval is the second derivative times the squared length of the interval divided by 24:

$$\epsilon(\Delta D) = \frac{1}{24}X_m\omega_L^2\bar{t}^2. \quad (50)$$

31 TOTAL ASTROMETRIC ERROR

31.1 Introduction

In this section it will be necessary to combine the effects from all the other error terms in this document, and look for inter-dependencies between different error terms.

31.2 Dependencies

The fundamental error calculation for the angular separation τ between two stars at direction vectors $\mathbf{s}_1$ and $\mathbf{s}_2$ is summarized follows: let a baseline vector $\mathbf{b}$ be given that at the same time specifies the x-coordinate of a Cartesian coordinate system. The zenith angles z_i and azimuth angles A_i of the two stars could be defined relative to the baseline vector:

$$\mathbf{s}_i = \begin{pmatrix} \cos A_i \sin z_i \\ \sin A_i \sin z_i \\ \cos z_i \end{pmatrix}; \qquad \mathbf{b} = \begin{pmatrix} b \\ 0 \\ 0 \end{pmatrix}. \tag{51}$$

The star separation becomes

$$\cos\tau = \mathbf{s}_1 \cdot \mathbf{s}_2 = \sin z_1 \sin z_2 \cos(A_1 - A_2) + \cos z_1 \cos z_2, \tag{52}$$

which for small separations Δz and ΔA

$$z_1 \equiv \bar{z} - \Delta z/2;\ z_2 \equiv \bar{z} + \Delta z/2;\ A_1 \equiv \bar{A} - \Delta A/2;\ A_2 \equiv \bar{A} + \Delta A/2; \tag{53}$$

is to lowest order in Δz and ΔA (see Section 28.3.5)

$$\tau^2 = (\Delta z)^2 + \sin^2\bar{z}(\Delta A)^2 + \cdots \tag{54}$$

The two OPD's are $\mathbf{s}_1 \cdot \mathbf{b} = b\cos A_1 \sin z_1$ and $\mathbf{s}_2 \cdot \mathbf{b} = b\cos A_2 \sin z_2$, and the ratio of the differential OPD $\Delta D \equiv D_1 - D_2$ over the baseline length b is

$$\frac{\Delta D}{b} = \cos A_1 \sin z_1 - \cos A_2 \sin z_2 \approx \sin\bar{A}\sin\bar{z}\Delta A - \cos\bar{A}\cos\bar{z}\Delta z. \tag{55}$$

Assuming that we know the direction of the SS relative to the PS parametrized by an angle φ,

$$\tau\sin\varphi \equiv \sin\bar{z}\Delta A; \qquad \tau\cos\varphi \equiv \Delta z, \tag{56}$$

the angle τ is related to the measured $\Delta D/b$ via

$$\tau = \frac{\Delta D}{b}\,\frac{1}{\sin\bar{A}\sin\varphi - \cos\bar{A}\cos\bar{z}\cos\varphi}. \tag{57}$$

Fig. 47 visualizes this geometry for a case $\Delta A > 0$ and $\Delta z > 0$: In the spherical right triangle with corners at the PS and the SS, the horizontal base that starts at the SS has a length of $|\Delta A \sin\bar{z}|$, the other cathetus has a length of Δz, and the hypotenuse has a length of τ. φ is the angle at PS between the meridian and the direction to the SS.

As a consequence of (57), observations at times that move the stars to alt-az positions (measured relative to the baseline direction) that are close to the pole of the fraction ought be avoided. This is detailed in Sec. 28. In more generic, qualitative interferometric terms the argument is that the

Another page of the PRIMA error budget [23] shows an example of the `http://www.strw.leidenuniv.nl/~mathar/prima/prErrWeb.html` GUI:

28.3.4 Numerical Simulator

More thorough numerical examples can be computed by the Java applet we provide in the `prErrWeb.html` link of the URL `http://www.strw.leidenuniv.nl/~mathar/prima/`; this takes into account the correlations between OPD and baseline errors, allows to introduce errors in both degrees of freedom (τ and φ) of the reduction, etc (Fig. 46).

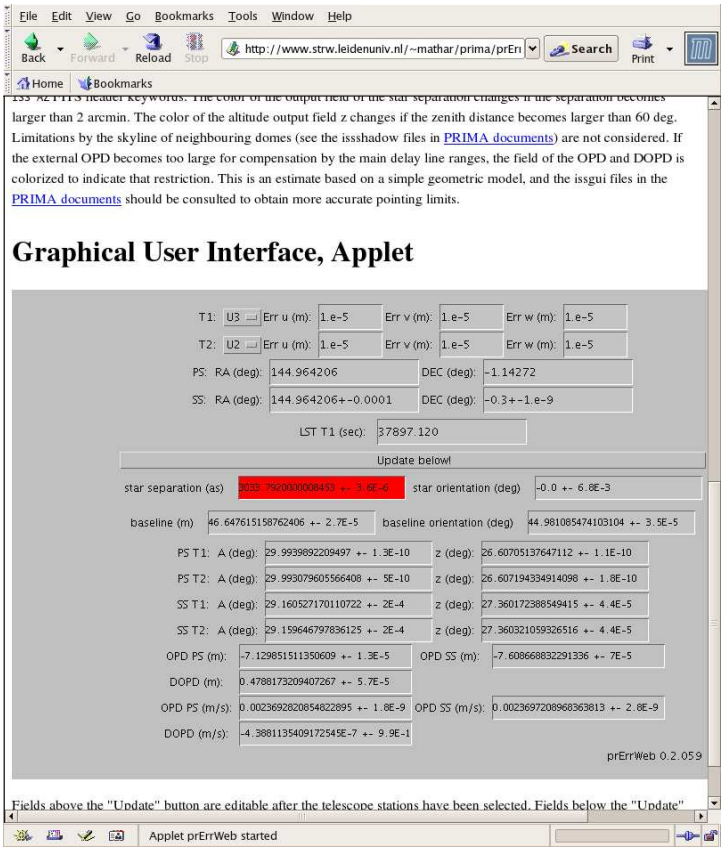

Figure 46: `prErrWeb.html` converts errors in station coordinates and star positions into errors of local sky coordinates and optical path differences.

ΔD can be rewritten in terms of $\Delta\delta$ and Δh of the star coordinates as in [103, §2.3].

APPENDIX F: EXTRACT OF ARXIV:ASTRO-PH/0411384

To point at a derivation of equation (12), a related page of [14] is reproduced here. The full text is available from `http://arXiv.org/abs/astro-ph/0411384`.

rad, for instance. The baseline angle in Eq. (3) becomes

$$\cos Z = \sin\Phi_1 \sin\Phi_2 + \cos\Phi_1 \cos\Phi_2 \cos(\Delta\lambda), \tag{59}$$

where $\Delta\lambda \equiv \lambda_1 - \lambda_2$. To transform Cartesian coordinates from the local alt-az-system of telescope i (with the Cartesian coordinate z pointing to the zenith, x horizontally tangentially to the earth toward north and the local horizon as indicated by the dotted line in Fig. 2, y horizontally toward west) to the geocentric system (with z pointing from the earth center to the north pole, x from the center to the equator south of Greenwich, y from the center to the equator 1000 km west of Sumatra) we translate the coordinates into a tilted system originating from the earth center, then (de)rotate them:

$$\mathbf{r}_c = \begin{pmatrix} -\sin\Phi_i\cos\lambda_i & \sin\lambda_i & \cos\Phi_i\cos\lambda_i \\ -\sin\Phi_i\sin\lambda_i & -\cos\lambda_i & \cos\Phi_i\sin\lambda_i \\ \cos\Phi_i & 0 & \sin\Phi_i \end{pmatrix} \cdot \left(\mathbf{r}_i + \begin{pmatrix} 0 \\ 0 \\ \rho \end{pmatrix} \right), \quad i = 1, 2. \tag{60}$$

The inverse operation with the inverse matrix (which equals the transpose matrix) is

$$\mathbf{r}_i = \begin{pmatrix} -\sin\Phi_i\cos\lambda_i & -\sin\Phi_i\sin\lambda_i & \cos\Phi_i \\ \sin\lambda_i & -\cos\lambda_i & 0 \\ \cos\Phi_i\cos\lambda_i & \cos\Phi_i\sin\lambda_i & \sin\Phi_i \end{pmatrix} \cdot \mathbf{r}_c - \begin{pmatrix} 0 \\ 0 \\ \rho \end{pmatrix}. \tag{61}$$

The product of two such operations with indexes 1 and 2 converts the two alt-az systems: starting in Eq. (60) with $\mathbf{r}_2 = 0$, computing $\mathbf{r}_c$, and inserting this into (61) for $i = 1$ shows that the origin of coordinates of telescope 2 is located at

$$\mathbf{b}_{12} = \rho \cdot \begin{pmatrix} -\sin\Phi_1\cos\Phi_2\cos(\Delta\lambda) + \cos\Phi_1\sin\Phi_2 \\ \cos\Phi_2\sin(\Delta\lambda) \\ \cos\Phi_1\cos\Phi_2\cos(\Delta\lambda) + \sin\Phi_1\sin\Phi_2 - 1 \end{pmatrix}$$

seen from the origin of telescope 1. The length of this vector is $b = |\mathbf{b}_{12}|$ of Eq. (3), using Eq. (59); the third coordinate is negative since the second telescope lies below the horizon of the first telescope (and vice versa), as illustrated in Fig. 2.

2.2.2. Vacuum limit

If the atmosphere is absent, the star direction is defined as

$$\mathbf{s}_i = \begin{pmatrix} \cos A_i \sin z_i \\ \sin A_i \sin z_i \\ \cos z_i \end{pmatrix}, \qquad i = 1, 2, \tag{62}$$

in terms of the true local azimuth A_i and true zenith angle z_i in the ith telescope coordinate system. A is counted positive starting from N to W. [This azimuth convention is the one of (Smart 1949, §II); the alternative convention of (Taff 1980; Karttunen et al. 1987) is obtained with the replacement $A_i \to \pi - A_i$.] The cosine of the angle between the star and the baseline in Fig. 2 is

$$\cos\varphi_1 = \mathbf{s}_1 \cdot \mathbf{b}_{12}/b, \tag{63}$$

where $\mathbf{s}_1 \cdot \mathbf{b}_{12}$ is known as the geometric optical path delay. If one swaps the indexes 1 and 2, the cosine switches its sign, because in this parallax-free situation the angle between star and baseline is the 180°-complement of the angle relative to the other telescope:

$$\cos\varphi_2 = \mathbf{s}_2 \cdot \mathbf{b}_{21}/b = -\cos\varphi_1. \tag{64}$$

This may be verified with the standard coordinate transformations between the hour angles h_i and right ascension δ for $i = 1, 2$,

$$\cos\delta \sin h_i = \sin z_i \sin A_i, \tag{65}$$

$$\sin z_i \cos A_i = \cos\Phi_i \sin\delta - \sin\Phi_i \cos\delta \cos h_i, \tag{66}$$

$$\cos z_i = \sin\Phi_i \sin\delta + \cos\Phi_i \cos\delta \cos h_i, \tag{67}$$

$$h_1 - h_2 = \lambda_1 - \lambda_2 \tag{68}$$

So if the atmosphere is absent, this angle relates to $P = |\sin\varphi_i| b$ $(i = 1, 2)$ as shown in Fig. 3.

The mean and difference in the true zenith angles remain defined as in Eqs. (31) and

$$\Delta z \equiv z_1 - z_2, \tag{69}$$

and can be retrieved from the geographical coordinates (66)–(67) and (Abramowitz & Stegun 1972, (4.3.34)-(4.3.37)).

APPENDIX G: SOFTWARE PROBLEM REPORTS

1. VLTSW20050024

```
Display VLT SPR VLTSW20050024                [Image] Help - [Image] Logout

Field Label     Field Value
Problem Number  VLTSW20050024
Originator      ssandroc
Location        ESO Paranal
Type            change request
Create-date     2005/01/25 16:50:54
Responsible     vltsccm
Package         TCS Telescope Control System (kwirenst gchiozzi awalland
                rkarban)
Priority
Status          open
Closed Status
Module Name     tcs
Module Version  1.147
cc              rkarban jargomed jspyromi
Synopsis        GPS + geographical positions
cc filter       rkarban jargomed jspyromi
Description     The geographical positions used by TCS should be updated.
                Based on the GPS timeserver values as input, the following
                table can be calculated.
                Compared to the previous values (taken from the VLT
                whitebook) the difference is about +6.5 arcsec (or 200 m)
                in both directions.

                GPS-Timeserver:
                Longitude Latitude
                d m s rad d m s rad
                TS 70 24 18.948 1.228803656 -24 37 41.634 -0.429843732

                Unit Telescopes:
                Longitude Latitude
                d m s rad d m s rad
                UT1 70 24 18.27 1.228800386 -24 37 39.44 -0.429833092
                UT2 70 24 17.39 1.228796107 -24 37 37.80 -0.429825122
                UT3 70 24 16.32 1.228790929 -24 37 36.64 -0.429819523
                UT4 70 24 14.25 1.228780856 -24 37 37.36 -0.429823005

                Auxiliary Telescope Stations:
                Longitude Latitude
                d m s rad d m s rad
                A0 70 24 18.44 1.228801200 -24 37 40.59 -0.429838653
                A1 70 24 18.26 1.228800303 -24 37 41.08 -0.429841025
                B0 70 24 18.17 1.228799896 -24 37 40.50 -0.429838245
                B1 70 24 17.99 1.228798998 -24 37 40.99 -0.429840617
                B2 70 24 17.89 1.228798549 -24 37 41.24 -0.429841803
                B3 70 24 17.80 1.228798100 -24 37 41.48 -0.429842989
                B4 70 24 17.71 1.228797651 -24 37 41.73 -0.429844175
                B5 70 24 17.62 1.228797202 -24 37 41.97 -0.429845361
                C0 70 24 17.90 1.228798591 -24 37 40.42 -0.429837837
                C1 70 24 17.72 1.228797693 -24 37 40.91 -0.429840209
                C2 70 24 17.63 1.228797244 -24 37 41.15 -0.429841395
                C3 70 24 17.53 1.228796795 -24 37 41.40 -0.429842581
                D0 70 24 17.36 1.228795981 -24 37 40.25 -0.429837021
                D1 70 24 16.99 1.228794186 -24 37 41.23 -0.429841765
                D2 70 24 16.81 1.228793288 -24 37 41.72 -0.429844137
                E0 70 24 16.83 1.228793372 -24 37 40.08 -0.429836204
                G0 70 24 16.29 1.228790762 -24 37 39.91 -0.429835388
                G1 70 24 15.55 1.228787171 -24 37 41.87 -0.429844877
                G2 70 24 16.57 1.228792109 -24 37 39.18 -0.429831830
                H0 70 24 15.21 1.228785543 -24 37 39.58 -0.429833756
                I1 70 24 14.48 1.228781994 -24 37 40.72 -0.429839279
                J1 70 24 14.13 1.228780282 -24 37 40.06 -0.429836090
                J2 70 24 13.85 1.228778935 -24 37 40.79 -0.429839649
                J3 70 24 15.05 1.228784771 -24 37 37.61 -0.429824230
                J4 70 24 15.24 1.228785668 -24 37 37.12 -0.429821857
                J5 70 24 15.52 1.228787015 -24 37 36.39 -0.429818299
                J6 70 24 15.79 1.228788362 -24 37 35.65 -0.429814741
                K0 70 24 14.14 1.228780324 -24 37 39.24 -0.429832124
                L0 70 24 13.87 1.228779019 -24 37 39.16 -0.429831716
                M0 70 24 13.60 1.228777714 -24 37 39.07 -0.429831308

Worklog
Last-modified-by
Modified-date
```

```
Status History
 Status   Modified-Time    Modified-By
 open  2005/01/25 16:50:54 ssandroc
```

Note that λ used here has the opposite sign to what has been used in the SPR reproduced above.

2. VLTSW20060066

```
From ARSystem@eso.org  Wed Apr  5 18:45:50 2006
Return-Path: <ARSystem@eso.org>
Date: Wed, 5 Apr 2006 18:45:11 +0200 (MEST)
From: ARSystem <ARSystem@eso.org>
Reply-To: ARSystem <ARSystem@eso.org>
To: mathar@strw.leidenuniv.nl
Subject: Remarks added to VLTSW20060066

Remarks have been made, see below for details

Problem Number : VLTSW20060066
Originator     : mathar
Responsible    : vltsccm
Priority       :
Package        : VLTI-ISS (awalland nhousen )
Module Name    : isstrkws
Module Version : 3.4
Type           : sw error
Location       : Leiden Observatory
Closed Status  :
cc             : pgitton,ott@four-d.de
Sysnopsis      : unexpected values of ISS PBLAij
Description    : The calculation of PBLAij in the isstrkws seems to be either in error
   or poorly documented. The actual calcuation projects the straight
   projected baseline vector (difference between the baseline vector and
   the delay vector into the star direction) onto the UV coordinate system
   and calculates some sort of azimuth angle (w.r.t. the horizontal
   West-South coordinate system). Most people in the interferometric community
   would expect to get the position angle discussed
   in section IIC of
   http://www.strw.leidenuniv.nl/~mathar/public/matharMIDI20051110.pdf
Worklog        :
   02/27/06 18:35:51     awalland
      The PBLAij has been implemented according to SPR VLTSW20040333.
      This SPR has been triggered by AMBER consortia and no complains have been raised
      after this implementation. Please consult AMBER consortia and agree on a different
      algorithm if that is required.
      The algorithm is given by Philippe Gitton and reproduced below.



      Calculation of the angle between the projected baseline vector wrt North direction
      ================================================================================
      GIP - May 10, 2005


      The reference frame used is defined as
       *  -> X along East
       *  -> Y along North
       *  -> Z along Zenith

       Let's define two vectors:

       Unit vector star defining the direction in which the telescopes point at
       using VLT convention:
        AZ = 0 when pointing south
        AZ = 90 when pointing east

      star[0] = sin(az)*cos(alt);
      star[1] = -cos(az) *cos(alt);
      star[2] = sin(alt);

      /* Baseline vector from TEL 1 to TEL 2 in units of meters */
      baseline[0] = coordTEL2[0] - coordTEL1[0];
      baseline[1] = coordTEL2[1] - coordTEL1[1];
      baseline[2] = coordTEL2[2] - coordTEL1[2];

      /* The sidereal OPD (sign being either positive or negative) is computed via: */
      sidOPD = star[0]*baseline[0]+star[1]*baseline[1]+star[2]*baseline[2];
```

```
   /* The projected baseline vector ProjBaseline in meters is: */
   ProjBaseline[0] = baseline[0] - sidOPD x star[0];
   ProjBaseline[1] = baseline[1] - sidOPD x star[1];
   ProjBaseline[2] = baseline[2] - sidOPD x star[2];

   /* Angle theta from North to the projection in the North-East plane of the projected baseline
          angle = 0 if projection along North
          angle = 90 deg if angle along East   */

   theta = arctan(ProjBaseline[0]/ProjBaseline[1]);
```

03/03/06 15:54:16 mathar

The OIFITS data format explicitly specifies the direction of the (x,y) plane--
and therefore the (u,v) plane--that catches the wavefront: this plane is
orthogonal to the direction of propagation, *not* orthogonal
to the topocentric zenith direction. To get a correct representation of the
coordinates as x=cos(angle)*PBL, y=sin(angle)*PBL in OI_VIS tables
[or angle replaced by angle+180 or angle+90 which is not explicitly defined by
OIFITS], the software must absolutely *avoid* to set angle=PBLA as currently
provided.
Note also that the angle is not defined modulo 180 [as currently implemented
with the arctan()] but modulo 360 degrees, as implemented with an arctan2().
This is because the first and the second telescope
define a baseline vector, and the projected baseline vector switches
direction if these are swapped. This adds 180 degrees to the angle
that ought be computed, and is equivalent to a sign convention for OPD's.
[This is independent of the obscure "wall-based" sign convention used within
the VLTI software.]
Note in passing that the ARRAY[XYZ] values in the ARRAY_GEOMETRY table
produced by ISS are also not compatible with the OIFITS standard: according
to OI_FITS the X component would be the value projected to the Greenwich
meridian, and the Y component form a right-handed coordinate system with
the Z component where Z points to the North. So for Paranal at -70 deg
of longitude as in ESO ISS GEOLON (although some astronomers would wrongly
argue this is +70 deg) we would need ARRAYX>0 and ARRAYY<0 and
|ARRAYX|<|ARRAYY| to be compatible with OIFITS.

03/30/06 22:41:48 mathar

From Fabien.Malbet@obs.ujf-grenoble.fr Mon Feb 27 22:29:53 2006
Return-Path: <Fabien.Malbet@obs.ujf-grenoble.fr>
Date: Mon, 27 Feb 2006 22:29:35 +0100
From: Fabien Malbet <Fabien.Malbet@obs.ujf-grenoble.fr>
To: Richard Mathar <mathar@strw.leidenuniv.nl>
CC: Gerard Zins <gerard.zins@obs.ujf-grenoble.fr>,
Gilles Duvert <Gilles.Duvert@obs.ujf-grenoble.fr>
Subject: Re: Fwd: Remarks added to VLTSW20060066

Dear Richard,

I have forwarded your request to our software team. Can you tell us a
little bit more about the conventions you are using? I am in vacation
riught now and I cannot check but we try to comply with usual
conventions of optical and radio interferometry. Hopefully, Gilles
Duvert will be able to reply to you on this subject.

Cheers,
fabien.

From Gerard.Zins@obs.ujf-grenoble.fr Tue Feb 28 08:54:18 2006
Date: Tue, 28 Feb 2006 08:53:18 +0100
From: Gerard Zins <Gerard.Zins@obs.ujf-grenoble.fr>
To: Richard Mathar <mathar@strw.leidenuniv.nl>
CC: Fabien Malbet <Fabien.Malbet@obs.ujf-grenoble.fr>,
Gilles Duvert <Gilles.Duvert@obs.ujf-grenoble.fr>
Subject: Re: [Fwd: Fwd: Remarks added to VLTSW20060066]

Dear Richard,

Gilles is in vacation this week. I will discuss this point with him next
week, and we will keep you informed.

Best regards,

Gerard.

04/05/06 18:44:59 mathar

The computational steps towards the baseline orientation angle are,
following the first proposal of Section IIC of my reference given before :
1) Compute A, the star azimuth, which is zero if the star is geographically
South, +90 deg if the star is West of the observatory. This is equivalent
to ISS AZ.

2) Compute A_b, the baseline azimuth on the platform. This is the
time-independent azimuth of Tj in coordinates centered at Ti. It is zero

```
   if Tj is south of Ti, +90 deg if Tj is West of Ti. This angle is
   approximately 180 degrees plus what is tabulated in
   http://www.eso.org/observing/etc/doc/vlti/baseline/baselinedata.txt .
   [We use only the difference between A_b and and A below, so both
   angles may be redefined with a different origin, for example a North=0
   convention. The common sense of orientation is mandatory, though.]
   Depending on the local programming conventions, this is some atan2()
   of the telescope coordinate differences North/South and East/West.

3) Compute/Get the star elevation above the horizon, a=90 deg minus z, where
   z is the star azimuth. This is equivalent to ISS ALT.
4) Compute the auxiliary angle psi, in C notation psi=atan2(sinpsi,cospsi),
   from the 2 intermediate variables  sinpsi=sin(A_b-A) and
   cospsi=cos(A_b-A)*sin(a) ... of course using radians instead of degrees.
   This implements Eqs. (35) and (36) of the current version of the reference.
5) Compute the parallactic angle p in the standard convention (that is
   zenith angle North-over-East): Imagine the star, the zenith Z and the
   north celestial pole (NCP) marked on the celestial sphere. Define the line
   from the observer to the star as an axis of rotation. Rotation of
   the NCP by the angle p around the axis moves the NCP onto the great circle
   defined by Z and the star. Since this angle is defined "North-over-East",
   one needs a left-handed sign convention with the aforementioned axis.
   [We avoid a clockwise or counter-clockwise terminology here because this
   depends on whether one looks at the celestial sphere from the inside or
   from the outside. It is impossible to tell from the current definition
   within DIC.ISS whether this is ISS PARANG as currently implemented.]
6) Compute the final angle p_i=p+psi+180 deg and normalize to the
   range 0..360 deg. p_i = slaDranrm(p+psi+M_PI)*DRAD2DEG
   Use this as the header keyword.

There has been no statement on this subject by the AMBER team so far. The
update of the keyword description on PLBAij in the DIC.ISS would simply be

comment: projected baseline orientation angle
description:
    Let the projected baseline be the great semicircle on the
    celestial sphere that starts at T1, passes by the star, and ends
    at T2. Let a rotation axis point from the observer at the sphere
    center to the star. The keyword value is the angle that
    actively rotates the North Celestial Pole around this axis until
    it meets the semicircle. The sign of the angle is "North-over-East"
    as if one would impose a "left-handed" rule on this directed axis
    of rotation.

If, however, for historical reasons, anybody wants to keep the old
computation of the keyword, the DIC.ISS needs a much more precise definition
of the current implementation for the current PBLAij. Keep in mind that this
information will be used by people who have neither access to the ESO SPR
system to look up the Gitton proposal nor access to the source code of the
isstrkws CMM module:

comment : topocentric doubly projected baseline angle
description:
    Define a projected baseline vector vec(P) from the delay
    vector vec(D), which points into the star direction, and
    the baseline vector vec(Ti->Tj): vec(D)+vec(P)=vec(Ti->Tj).
    Project vec(P) on the topocentric plane defined by the
    observatory's horizon (ie, subtract its zenith component).
    The keyword value is some compass rose (=geographical)
    orientation, confined to the range [-90..90] degrees which
    means dropping this doubly projected baseline vector's
    sense of orientation.

Then, a new keyword for the standard projected baseline angle, like PBOAij,
(short for projected baseline orientation angle from i to j)
needs to be defined that is computed according to 1)-6), and gets the
ESO-VLT-DIC.ISS description mentioned first.
```

APPENDIX H: WEB PAGE CHANGE REQUEST

```
Your support request number WWW-22658 has now been closed. You will find the resolution at the END of this message.

Please contact us again quoting the above number should you find the resolution unsatisfactory.

Rgds.
ESO Web Team

Entry-Id                : WWW-22658
First Name              : Email
Last Name               : User
```

```
Category                  : Non-Web Request
Short-Description         : vltistations.html
Problem Description       :
   02/27/06 13:10:21     mathar
      ------------------------------------------------------------------------
      MESSAGE FROM REMEDY
      This mail was CC to the following recipients:
      mathar@mail.strw.leidenuniv.nl
      ------------------------------------------------------------------------

      The angular values listed under the Pos.Angle column of
      http=//www.eso.org/observing/etc/doc/vlti/baseline/baselinedata.txt
      are not compatible with the GPS measurements of 2005 provided in the software
      problem report VLTSW20050024. An updated list is available from the
      appendix of
      http=//www.strw.leidenuniv.nl/~mathar/public/matharMIDI20051110.pdf .
      The deviations are 0.05 degrees for the first entry, A0-B0, for example.
      See also VLTSW20060051.

      ========================================================================
      Richard J Mathar                Tel (+31) (0) 71 527 8459
      Sterrewacht Universiteit Leiden Fax (+31) (0) 71 527 5819
      Postbus 9513
      2300 RA Leiden                  E-mail mathar@strw.leidenuniv.nl
      The Netherlands                 URL http=//www.strw.leidenuniv.nl/~mathar
Server/Cluster            : Observing
Resolution                :
   02/27/06 13:58:17     srahimpo
      Thank you for your e-mail. Unfortunately, the ESO Web Team is not
      able to take care of your request. Below you can find a list of contact addresses
      for particular problems.

      In order to obtain support and reply to your question/request, you
      may contact one of the following e-mail addresses.

      - For matters related to Phase 2 Observing Proposal preparation and
        submission, please contact the ESO User Support Group via
        <usd-help@eso.org>;
      - For information concerning observing trips to La Silla and Paranal,
        contact the Section Visiting Astronomer <visas@eso.org>;
      - For matters related to the ESO Archive, please contact the ESO
        Archive Group via <catalog@eso.org>;
      - For matters related to the Remedy Action Request System, please
        contact the ESO Remedy Team via <remedy@eso.org>.

      Kind regards,
        The ESO Web Team
```

APPENDIX I: ACRONYMS

ARAL Artificial Source and Alignment Toolkit

AT Auxiliary Telescope (of the VLTI) `http://www.eso.org/projects/vlti/AT/index_at.html`

DL Delay Line `http://www.eso.org/outreach/press-rel/pr-2000/phot-26-00.html`

DLMT Delay Line Mirror Translation Stage (of the MIDI warm optics)

eclipse ESO C Library for an Image Processing Software Environment `http://www.eso.org/eclipse`

ESO European Southern Observatory `http://www.eso.org`

EWS Expert Work Station (of MIDI)

FITS Flexible Image Transport System `http://fits.gsfc.nasa.gov`

fv fits viewer `http://heasarc.gsfc.nasa.gov/docs/software/ftools/fv/`

GUI Graphical User Interface

ISS Interferometric Supervisor-Software

MDL main delay line

MIA MIDI Interactive Analysis `http://www.strw.leidenuniv.nl/~koehler/MIDI/`

MIDI Mid-Infrared Interferometric Instrument http://www.mpia.de/MIDI

MPIA Max-Planck Institut für Astronomie, Heidelberg http://www.mpia.de

NCP North Celestial Pole

OIFITS Optical Interferometry FITS Exchange Format http://www.mrao.cam.ac.uk/~jsy1001/exchange/

OPD optical path difference

OPL optical path length

P2PP Phase 2 Proposal Preparation http://www.eso.org/observing/p2pp

PRIMA Phase-Reference Imaging and Microarcsecond Astrometry
http://obswww.unige.ch/Instruments/PRIMA

PSF point spread function

SCP South Celestial Pole

SPR Software Problem Report http://www.eso.org/vlt/sw-dev

SWY switchyard (table in the VLTI lab)

UT Unit Telescope (of the VLTI) http://www.eso.org/projects/vlt/unit-tel/

VLTI Very Large Telescope Interferometer http://www.eso.org/vlti

ZOPD zero OPD

APPENDIX J: NOTATIONS

α	right ascension
a, a'	star elevation; inclination of projected baseline plane towards horizontal
A, ΔA; A_b; A_λ	star azimuth angle, and its change; baseline azimuth; visibility amplitude
$b, \mathbf{b}_{12}$	baseline length and vector
d	aperture diameter
δ	declination
D, D_a, D_i	OPD
ϕ	field rotation angle
Φ	geographical latitude
φ	angular phase shift
h	hour angle
L	path length
λ	wavelength; geographical longitude
p	parallactic angle
p_i	positional angle of the projected baseline circle
P	projected baseline
ρ	Earth radius
$\mathbf{s}$	unit vector into star direction
θ	angular separation between pointing and baseline vector
t	time
τ	baseline position angle
U, V, W	Paranal Cartesian coordinates
ψ	intersection angle between projected baseline circle and star meridian
z, Δz	zenith angle, differential zenith angle
Z	baseline angle seen from the Earth center

[1] Abramowitz, M., and I. A. Stegun (eds.), 1972, *Handbook of Mathematical Functions* (Dover Publications, New York), 9th edition, ISBN 0-486-61272-4.
[2] Adams, D., 1995, *A Hitch Hikers Guide To The Galaxy* (Ballantine Books), ISBN 0-345-391802.
[3] Ballester, P., and C. Sabet, 2002, *VLT Interferometer VLTI Data Interface Control Document*, VLT-SPE-ESO-15000-2764.
[4] Boden, A. F., 2000, in *Principles of Long Baseline Stellar Interferometry*, edited by P. R. Lawson (National Aeronautics and Space Administration), p. 9, jPL publication 00-009 07/00.
[5] Calbretta, M. R., and E. W. Greisen, 2002, Astron. & Astrophys. **395**, 1077.
[6] Galliano, E., M. Schöller, M. Fischer, C. Hummel, S. Morel, F. Rantakyrö, and M. Vannier, 2004, in *New Frontiers in Stellar Interferometry*, edited by W. A. Traub (Int. Soc. Optical Engineering), volume 5491 of *Proc. SPIE*, pp. 1540–1548.
[7] Gitton, P., 2003, Re: north angle, priv. commun.
[8] Gitton, P., 2006, Re: VLT ICD question, priv. commun.
[9] Gitton, P., R. Wilhelm, A. Glindemann, and F. Paresce, 2003, *Determination of the field and pupil rotation in the VLTI laboratory*, VLT-TRE-ESO-15000-3092.
[10] Glazenborg, A., 2002, *MIDI Optical Design of the Cold Bench*, VLT-SPE-MID-15821-0101.
[11] Harries, F. E., 1963, Rev. Mod. Phys. **35**(3), 558.
[12] Jaffe, W. J., 2004, in *Astronomical Telescopes and Instrumentation*, edited by W. A. Traub (Int. Soc. Optical Engineering), volume 5491 of *Proc. SPIE*, pp. 715–725.
[13] Leinert, C., 2003, Transfer of V, W-"field" onto MIDI, priv. commun.
[14] Mathar, R. J., 2004, arXiv:astro-ph/0411384 .
[15] Mathar, R. J., 2004, *MIDI Observation Software, User and Maintenance Manual*, VLT-TRE-MID-15824-0264.
[16] Mathar, R. J., 2005, Baltic Astronomy **14**(2), 277.
[17] Morel, S., 2006, *MIDI User Manual*, VLT-MAN-ESO-15820-3519.
[18] Pauls, T. A., J. S. Young, W. D. Cotton, and J. D. Monnier, 2004, in *New Frontiers in Stellar Interferometry*, edited by W. A. Traub (Int. Soc. Optical Engineering), volume 5491 of *Proc. SPIE*, pp. 1231–1239.
[19] Pel, J.-W., 1999, *MIDI Preliminary alignment plan*, VLT-TRE-MID-15821-0107.
[20] Puech, F., and P. Gitton, 2005, *Interface Control Document between VLTI and its Instruments*, VLT-ICD-ESO-15000-1826.
[21] Smart, W. M. (ed.), 1949, *Text-book on Spherical Astronomy* (Cambridge University Press, Cambridge).

[22] Stanghellini, S., and A. Michel, 1998, The Messenger **94**, 10.
[23] Tubbs, R. N., and R. J. Mathar, 2006, *Astrometric Survey for Extra-Solar Planets with PRIMA, Astrometric Error Budget*, VLT-TRE-AOS-15753-0001.
[24] Wallander, A., 2005, *ICD between VLTI Supervisor SW and VLTI Instrumentation SW*, VLT-ICD-ESO-15410-2117.
[25] Wilhelm, R., B. Koehler, and P. Gitton, 2002, *Functional Description of the VLTI*, VLT-ICD-ESO-15000-1918. The radii of curvature of M2, M5 and M7 in Table 4-1 are wrong. See [22] for M2.